AD-A126 433 CIRCULATION AND SHOALING STUDY OF THE PORT OF ASTORIA (U) OREGON STATE UNIV CORVALLIS DEPT OF CIVIL ENGINEERING R S GUSTAIN DEC 82 1/1

UNCLASSIFIED F/G 8/8 NL

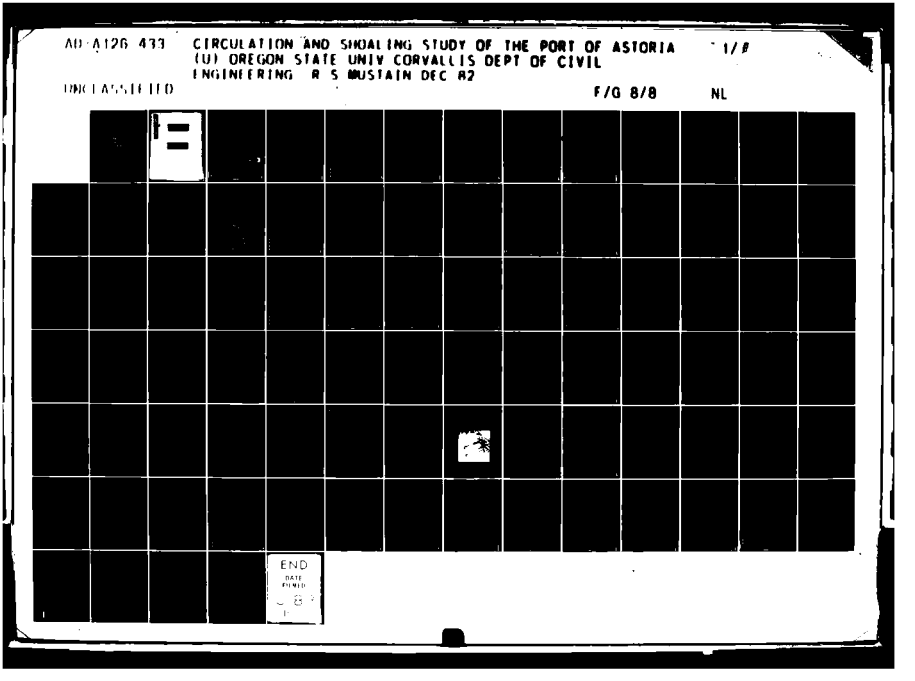

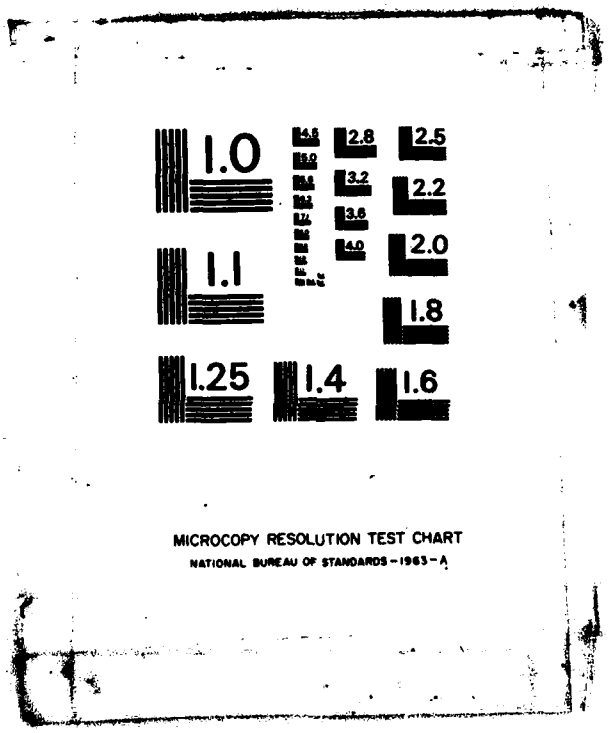

MICROCOPY RESOLUTION TEST CHART
NATIONAL BUREAU OF STANDARDS-1963-A

AD A126433

Circulation and Shoaling Study of the Port of Astoria

by
Roger S. Mustain
LT, CEC, USNR

Circulation and Shoaling Study of the Port of Astoria

by
Roger S. Mustain
LT, CEC, USNR

Dec. 1982

A Project
Submitted to
Oregon State University

in partial fulfillment of the
requirements for the degree of
Master of Science

DTIC
ELECTE
APR 6 1983
D
A

OREGON WATER RESOURCES RESEARCH.

This document has been approved for public release and sale; its distribution is unlimited.

Acknowledgements

More people rendered me assistance on this project than I can reasonably thank here. However, I would like to express my particular gratitude to some who stand out in my recollection. In particular, Professor Bill McDougal, who allowed me to use his numerical circulation model and who provided frequent assistance, comments, and guidance on the other aspects of the project and Professor Larry Slotta for his guidance and encouragement throughout the project. Also, my fellow students who collaborated on the project, notably Don Carlos Cobos, Rick Morris and Jim Hanson.

Finally, I must express my appreciation to the United States Navy for making it possible for me to attend postgraduate school.

R. S. Mustain
LT, CEC, USNR
December, 1982

Accession For
NTIS GRA&I ☑
DTIC TAB ☐
Unannounced ☐
Justification
Per Ltr on file
By
Distribution/
Availability Codes
Dist | Avail and/or Special
A

DTIC COPY INSPECTED 3

Table of Contents

List of Tables

List of Figures

I. Introduction

The ports on the lower Columbia River have historically experienced moderate shoaling problems. Recently, however, the rate of shoaling has increased sharply, apparently as a result of the volcanic activity of Mt. St. Helens in May 1980, and again in March 1982. The Port of Astoria was seriously affected. The annual volume of dredging required to maintain the harbor slips in a usable condition more than doubled, exceeding the capacity of the existing dredging equipment. The Port subsequently requested some $500,000 from the State of Oregon's Emergency Fund to offset its increased dredging costs.

A significant concern is whether the severe sedimentation currently being experienced will prove to be a relatively short term phenomenon, or whether the severe condition may become chronic. If the latter, long term solutions other than emergency dredging should be considered.

The research reported herein was commenced in October of 1981 with the following objectives:

(a) To determine the impact of the Mt. St. Helens eruptions on the shoaling problem.

(b) To identify the causes of shoaling in the ports along the Columbia River estuary.

(c) To estimate the long term effects of the Mt. St. Helens eruptions.

The scope of the study was limited to the Port of Astoria and environs due to budget constraints. However, the results of the study would, hopefully, provide relevant information concerning the problems experienced by other ports in the area.

This paper deals primarily with objective (b) of the overall study. Specifically, the objective of this paper is to develop an understanding of the circulation patterns of currents in the vicinity of the harbor slips at the Port of Astoria. Such an understanding is a necessary prerequisite to conducting research into the mechanisms which cause sedimentation to occur.

The study used numerical and physical models to predict currents, circulation patterns and flushing rates for the port area. The models were followed up by a field study to verify the results of the simulations.

Finally, a numerical sedimentation model was considered in an attempt to estimate the rate of sedimentation in the harbor area.

B

II. Experimental Approach

The research presented in this paper was concentrated fairly heavily on the theoretical aspects of the subjects of sedimentation and hydraulic exchange at the Port of Astoria. This approach was adopted for two reasons. First, there was a lack of readily available information concerning the sediment (concentrations, distributions, and characteristics) and hydraulic behavior (velocities, flow patterns, etc.) in the vicinity of the Port of Astoria. Second, this project was relatively limited in the resources available to gather such information in the field.

Given these considerations, it was decided to thoroughly analyze the problem from several theoretical viewpoints in an effort to gain insights into the key processes which drive the system. If these key processes could be identified and understood, the resources available for field research and validation of theoretical results could then be optimally allocated to obtain the necessary data while avoiding wasted efforts.

The theoretical approach which was adopted involved the use of three separate modeling systems, each simulating various aspects of the hydraulic and/or sedimentary processes at the Port of Astoria. The models used were a small scale physical model (described in Section IV), a one-dimensional numerical circulation model (Section V) and a single-cell numerical sedimentation model (Section VI).

The physical model provided a simple visual interpretation of the flow patterns in the port area. This model was essentially qualitative in nature, that is, actual velocities, concentrations,

etc. were not measured and could only be roughly estimated from the photographic results.

The one-dimensional numerical circulation model provided quantitive estimates of the flushing characteristics and flow rates in the harbor. Additionally, average velocities along the axis of the harbor slips could be estimated based on the predicted flow rates.

The single-cell numerical sedimentation model was used to estimate the rate of sedimentation which would occur in the harbor slips.

Finally, a field study was conducted in an effort to validate the model results (details of the field study are given in Section VIII).

III. Prototype Charasteristics

A. Site Description

The Port of Astoria is located on the south bank of the Columbia River approximately 13 miles (21 Km) from the river mouth. The port is situated on a peninsula bounded by the Columbia River to the north, and Young's Bay to the west, as shown in fig. 1.

The industrial area of the port, as shown in fig. 2, comprises two slips, slip number one being the more easterly. Both slips are open at their north end to the Columbia River which has a depth of about 40 feet (12 m) in the vicinity of the port. The navigational channel of the Columbia passes within about 200 yards (180 m) of the harbor mouth.

The piers which form the sides of each slip have concrete decks supported by wood pilings. Beneath the deck, a rubble breakwater extends along the length of each pier, although in the case of pier number three, the breakwater does not extend the full length of the pier. Above the deck the piers are equipped with utilities, shop, office, and warehouse spaces, and tracks for rail-mounted cranes and/or railroad cars.

Slip number one is more heavily commercially utilized than slip number two, and consequently is more frequently and thoroughly dredged.

(Hamilton, 1973) Columbia River Estuary Figure 1

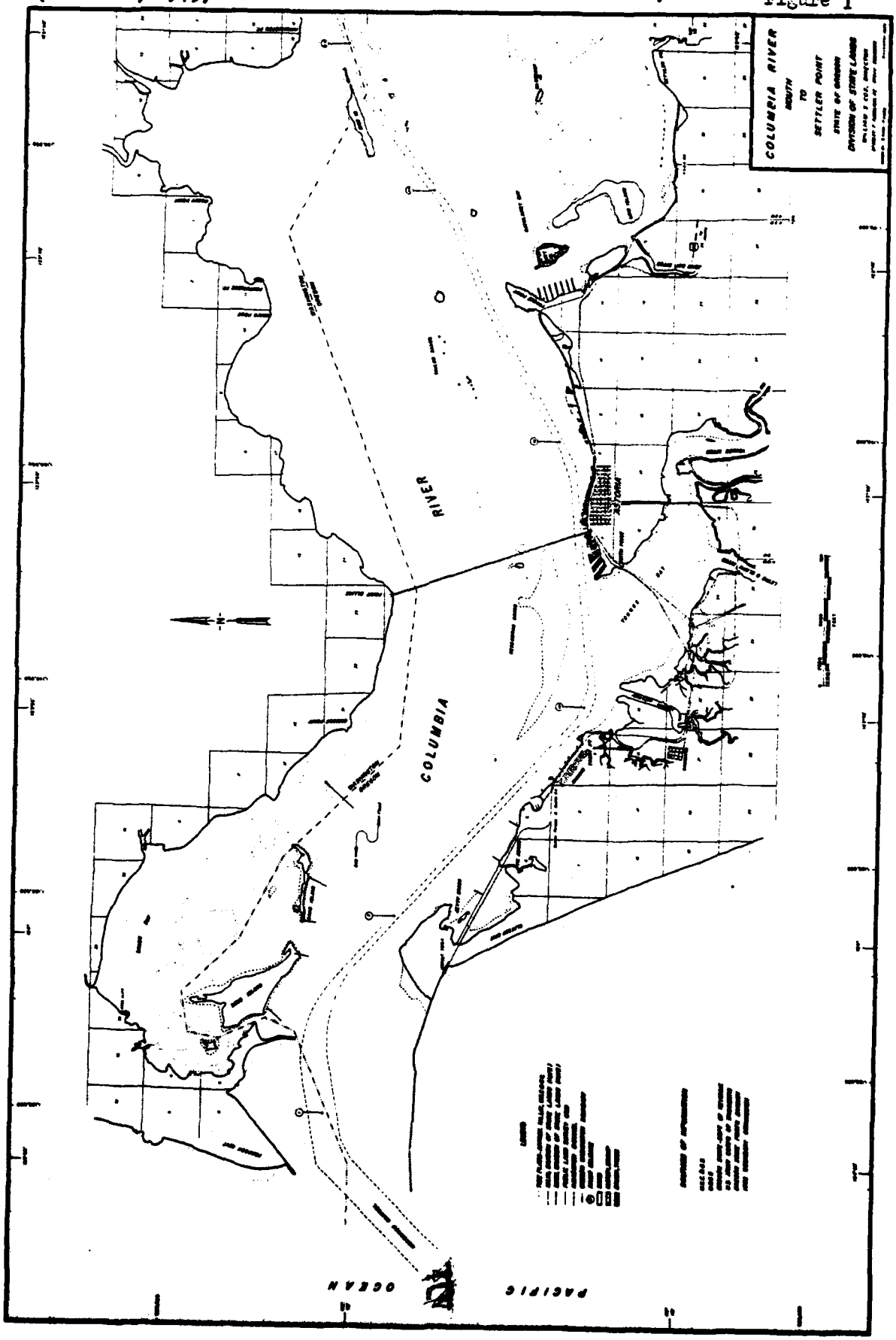

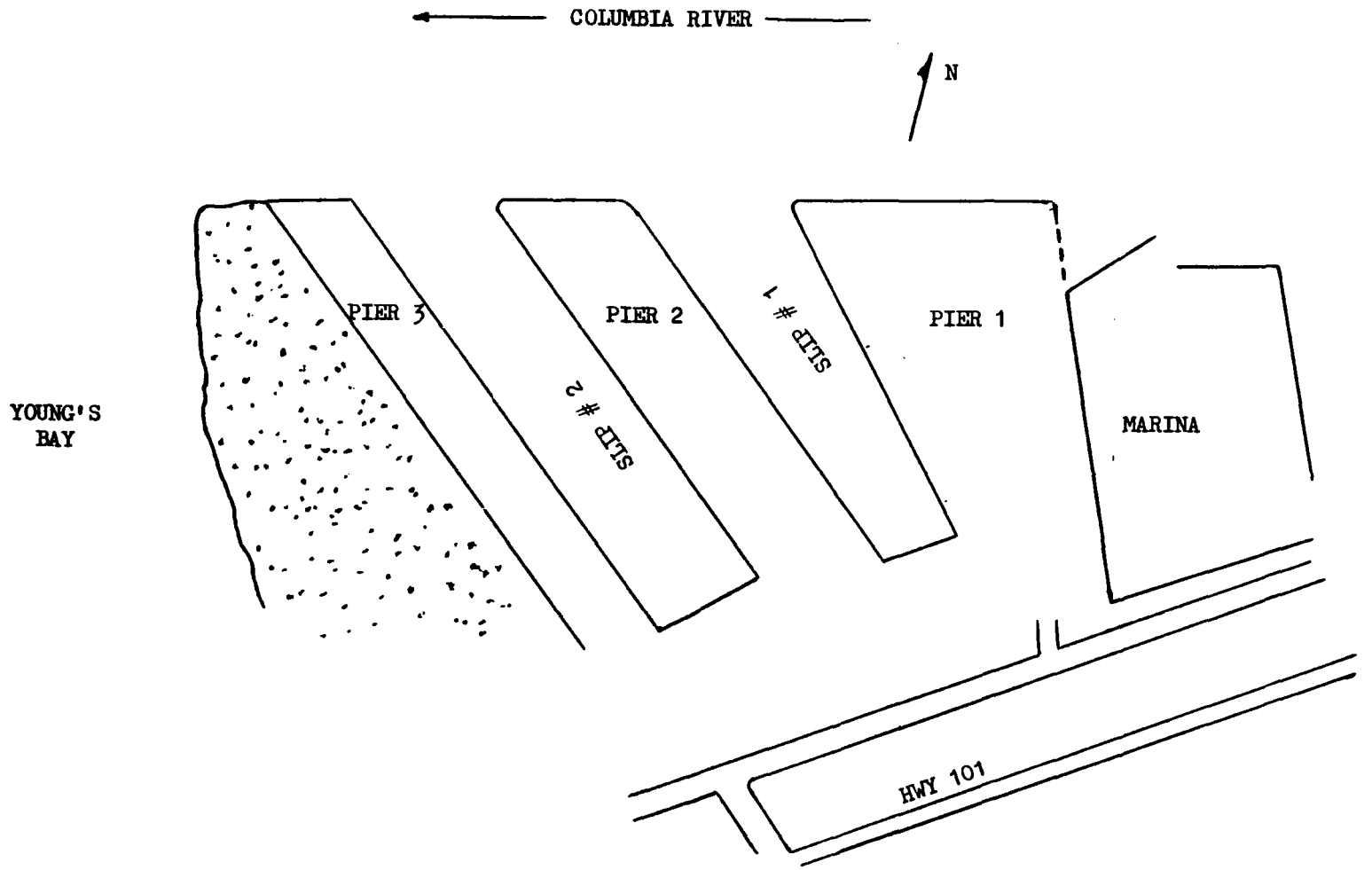

Figure 2 Port of Astoria, Oregon

An important activity at the port is loading timber, which is often towed into the port in the form of extensive log rafts and loaded directly from the water on board freighters.

The Port of Astoria has traditionally experienced moderate problems with sediment buildup in the slips. Prior to 1980, the average rate of sedimentation was about six feet per year. Since the eruption of Mt. St. Helens in May 1980, however, the rate of sedimentation has more than doubled, a matter of serious concern to the Port officials (Personal communication with the Port of Astoria).

B. Hydrology and Tidal Dynamics

The Columbia River is the largest river draining the Pacific Coast of North America. River discharge varies seasonally and is largely determined by two factors: local precipitation (highest during the winter) and snow melt (highest during late spring and summer). Additionally, river discharge is affected by dam regulation. Lowest discharge generally occurs during late summer and early fall, when both precipitation and snow melt are at a minimum. Average peak discharges for the ten year period 1966 to 1976 are as follows (Gelfenbaum, 1982):

Winter freshet: 384,000 ft^3/sec (10,900 m^3/s)

Spring freshet: 476,000 ft^3/sec (13,500 m^3/s)

Minimum Discharge: 137,000 ft^3/sec (3,900 m^3/s)

Figure 3 shows the monthly average discharges for water year 1980 (U.S. Geological Survey, 1981). Of particular interest are the winter and spring freshets, where the flow exceeds 300,000 cfs (9000 m^3/sec).

Figure 3

AVERAGE DISCHARGE AT THE COLUMBIA RIVER MOUTH, WATER YEAR 1980

(U. S. Geological Survey, 1981)

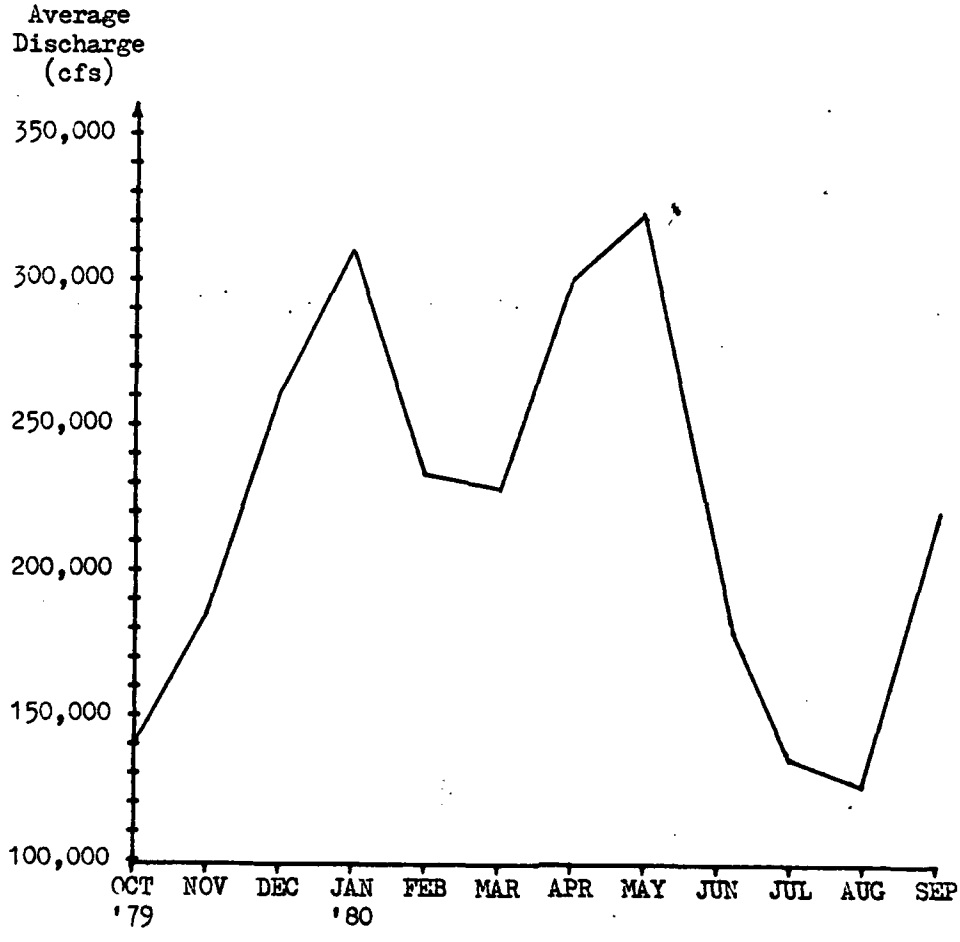

Note: 1 cfs = .028 m^3/sec

The suspended sediment load of the Columbia River varies with the total flow. During the winter and spring freshets, the sediment-carrying capacity of the river is greatly increased.

The lower reaches of the Columbia River form an extensive estuary, with an area of some 94,000 acres ($3.8 \times 10^8 m^2$) (Hamilton, 1973). Tidal fluctuations are observed as far upstream as Bonneville Dam, 140 miles (225 Km) from the mouth. Tidal flow reversals are observed about 53 miles (85 Km) up the river, while the limit of seawater intrusion is about 23 miles (37 Km).

The tides affecting the Columbia estuary are of a mixed semi-diurnal type typical to the Oregon Coast (see fig. 4). The mean tidal range at the mouth of the river is about 6.6 feet (2.0 m) with a maximum range during spring tides of 11.1 ft (3.4 m) (Neal, 1965, Dyer, 1973).

C. Sediments

The sediment in the Astoria area consists of land erosion products transported by the Young's, Lewis & Clark, and Columbia Rivers (Krone, 1971). The bed of the estuary is predominantly fine sand, with increasing amounts of silt and clay near the river banks and in sheltered areas such as Young's Bay. Within the slips at the Port of Astoria, the bed materials are predominantly silt and clay, becoming coarser and containing some fine sand near the slip's entrances.

An interesting feature of the Columbia estuary is the presence of a turbidity maximum. This phenomenon develops in some estuaries as a result of the circulation pattern, typically where there exists an upriver flow of dense salt water near the bottom

TIDAL ELEVATIONS ON THE OREGON COAST

STATE OF OREGON
DIVISION OF STATE LANDS

Typical Days Tide

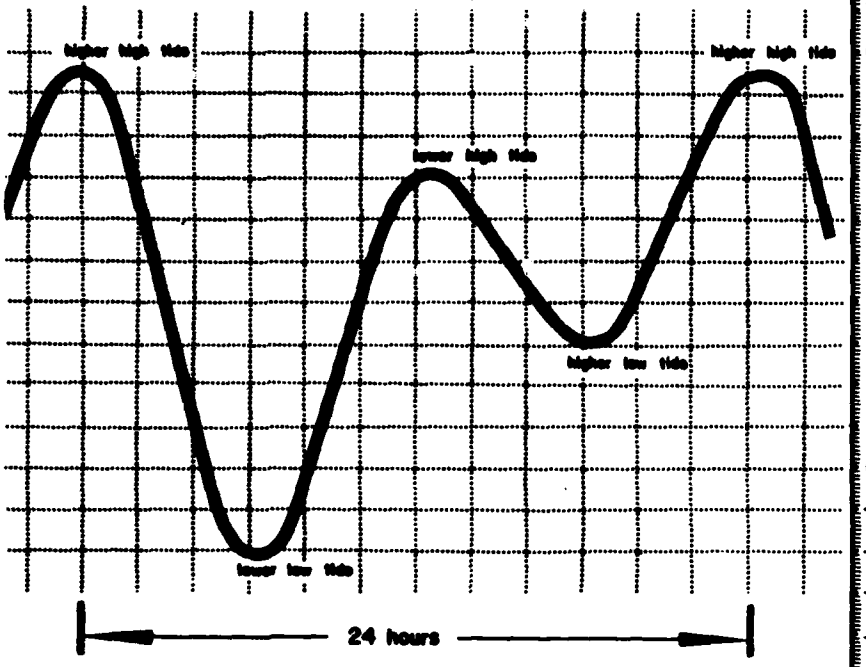

Note: Specific elevations are based on six years of tide observations at the Oregon State University Marine Science Center Dock on Yaquina Bay. Values have been reduced by the National Ocean Survey (formerly the Coast and Geodetic Survey). The elevations differ from estuary to estuary and from different points within an estuary. The exception is MLLW which is zero by definition.

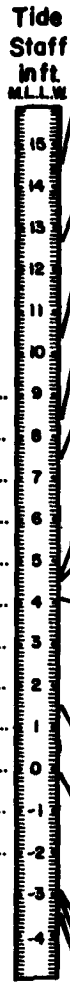

14.5 Extreme High Tide – The highest projected tide that can occur. It is the sum of the highest predicted tide and the highest recorded storm surge. Such an event would be expected to have a very long recurrence interval. In some locations, the effect of a rain induced freshet must also be taken under consideration. The extreme high tide level is used by engineers for the design of harbor structures.

12.63 Highest Measured Tide – The higest tide actually observed on the tide staff.

10.3 Highest Predicted Tide – Highest tide predicted by the Tide Tables.

8.38 Mean Higher High Water – The average height of the higher high tides observed over a specific time interval. The intervals are related to the moon's many cycles which range from 28 days to 18.6 years. The time length chosen depends upon the refinement required. The datum plane of MHHW is used on National Ocean Survey charts to reference rocks awash and navigational clearances.

7.62 Mean High Water – The average of all observed high tides. The average is of both the higher high and of the lower high tide recorded each day over a specific time period. The datum of MHW is the boundary between upland and tideland. It is used on navigational charts to reference topographical features.

4.58 Mean Tide Level – Also called half-tide level. A level midway between mean high water and mean low water. The difference between mean tide level and local mean sea level reflects the asymmetry between local high and low tides.

4.51 Local Mean Sea Level – The average height of the water surface for all stages of the tide at a particular observation point. The level is usually determined from hourly height readings.

4.11 Mean Sea Level – A datum based upon observations taken over a number of years at various tide stations along the west coast of the United States and Canada. It is officially known as the Sea Level Datum of 1929, 1947 adj. and is the most common datum used by engineers. MSL is the reference for elevations on U.S. Geological Survey Quandrangles. The difference between MSL and Local MSL reflects numerous factors ranging from the location of the tide staff within an estuary to global weather patterns.

1.54 Mean Low Water – The average of all observed low tides. The average is of both the lower low and of the higher low tides recorded each day over a specific time period. The datum of MLW is the boundary between tideland and submerged land.

0.00 Mean Lower Low Water – The average height of the lower low tides observed over a specific time interval. The datum plane is used on Pacific coast nautical charts to reference soundings.

-2.9 Lowest Predicted Tide – The lowest tide predicted by the Tide Tables.

-3.14 Lowest Measured Tide – The lowest tide actually observed on the tide staff.

-3.5 Extreme Low Tide – The lowest estimated tide that can occur. Used by navigational and harbor interests.

(Hamilton, 1973)

Tidal Elevations on the Oregon Coast

Figure 4

with an overlying downriver flow of less dense fresh water on the surface (Ippen, 1966). The location of the turbidity maximum in the Columbia estuary varies with the fresh water discharge and tidal condition. When high discharges occur in conjunction with low tides, the turbidity maximum is centered around river mile 9 (Km 15), while during low discharges and high tides, the turbidity maximum moves upstream as far as river mile 16 (Km 26). The Port of Astoria, located at river mile 13 (Km 21) is thus within the range of excursion of the turbidity maximum (Gelfenbaum, 1982). Concentrations of suspended sediments in the area of the turbidity maximum may be as high as 10 times the average suspended concentration in the estuary as a whole.

IV. Physical Model

A physical hydraulic model was used to conduct a preliminary investigation of the hydrodynamics and flushing in the port area. The model was of small size and not designed or intended to provide precise quantitative information in regard to velocities, flow rates, diffusivities, etc. Rather, the model was intended to provide a clear overview of the possible hydraulic exchanges occurring within the harbor slips. The information thus gained could then serve as a "point of departure" for further studies, either field or theoretical.

A. Theory of Hydraulic Similitude

The accuracy of any hydraulic model in predicting the behavior of its real counterpart (the prototype) depends on the degree to which the properties of the model, both fluid (i.e. viscosity, density, surface tension) and physical (i.e. geometry and roughness), reflect those of the prototype. This correspondence between the properties of the model and prototype is described by the theory of similitude.

One may refer to hydraulic similitude in terms of geometric, kinematic or dynamic similarity (ASCE, 1942).

(1) Geometrical similarity: two objects are said to be geometrically similar if the ratios of all corresponding (homologous) dimensions are equal. Thus, geometric similarity involves only similarity of form.

(2) Kinematic similarity: similarity of motion. Two motions are kinematically similar if the patterns or paths of motions are geometrically similar and if the ratios of the velocities of the various homologous particles involved in the motion occurrences are equal.

(3) Dynamic similarity: similarity of masses and forces. Two motions are dynamically similar if they are kinematically similar, the ratios of the masses of the various homologous objects involved in the motions are equal, and the ratios of the homologous forces which affect the motions are equal.

Complete dynamic similarity is an ideal which could only be attained using a model:prototype scale ratio of 1:1 if the same fluid were used in both. If a different fluid or medium is used in the model than in the prototype, a unique scale ratio would exist which would result in complete dynamic similarity (ASCE, 1942). However, in spite of the imperfectness of the dynamic similarity, a model of scale considerably smaller than 1:1 can provide meaningful results.

The hydrodynamic behavior of a tidal estuary constitutes a complex free surface problem. The flow is unsteady, non-uniform, and periodically reverses. In addition, the fluid may be non-homogeneous due to differences in salinity and temperature. Nevertheless, the motions which occur may be described by differential equations relating to momentum and mass transfer (Slotta and Tang, 1976). Although it may not be possible to solve these equations, they can be used to determine how the variables must be grouped in an equation describing the solution (Bennet and Myers, 1962).

Consider the Navier-Stokes equation for flow in the x-direction:

$$\frac{\partial U}{\partial t} + U_x\frac{\partial U_x}{\partial x} + U_y\frac{\partial U_x}{\partial y} + U_z\frac{\partial U_x}{\partial z} = g_x - \frac{1}{\rho}\frac{\partial p}{\partial x} + \nu\left(\frac{\partial^2 U_x}{\partial x^2} + \frac{\partial^2 U_x}{\partial y^2} + \frac{\partial^2 U_x}{\partial z^2}\right) \quad \text{(eq. 1)}$$

Where:
- u = velocity
- g = gravitational acceleration
- t = time
- p = pressure
- ρ = density
- ν = kinematic viscosity
- x, y, z subscripts denote direction in a Cartesian coordinate system

This equation is dimensionally homogeneous, i.e. all terms have the same dimensions, L/T^2.

Adopting the notations U_o for a characteristic velocity and L_o for a characteristic length, equation 1 can be rewritten in a dimensional form as:

$$\frac{U_o^2}{L_o} = g - \frac{p}{\rho L_o} + \frac{U_o}{L_o^2}\nu \quad \text{(eq. 2)}$$

Note that this equation represents only an equality of dimensions, not a mathematical equality. Equation 2 may be expressed in dimensionless form by dividing each term by U_o^2/L_o:

$$(1) = \frac{gL_o}{U_o^2} - \frac{g_o p}{U_o^2\rho} + \frac{\nu}{U_o L_o} \quad \text{(eq. 3)}$$

This equation gives the functional relationship between three dimensionless groups of numbers. The dimensionless groups are as follows.

$\frac{g_c p}{U_0^2 \rho}$ = Euler Number $\propto$ pressure forces / inertia forces (eq. 4)

$\frac{U_0^2}{g L_0}$ = Froude Number $\propto$ inertia forces / gravity forces (eq. 5)

$\frac{U_0 L_0}{\nu}$ = Reynolds Number $\propto$ inertia forces / viscous forces (eq. 6)

The Reynolds and Froude numbers are particularly significant when considering dynamic similitude. The Froude number is an important parameter when gravity exerts a significant influence on the fluid motion, that is, when a free surface is present. The Reynolds number is important when viscous forces affect the fluid motion. For exact dynamic similitude to occur, equality of both the Reynolds and Froude numbers between the prototype and model would have to exist. Given the limited range of kinematic viscosities of the liquids commonly available for modeling, this would require a scale ratio close to unity. As previously noted, the selection of a fluid (with a given ν) would result in a single proper scale ratio for the model.

Fortunately, in the case of modeling an estuary, the fluid motions are governed by gravitational forces, and fall into the

category of turbulent, high Reynolds number flow. Under these conditions, molecular viscosity effects vary only slightly as a function of the Reynolds number. Consequently, most estuarine models are dimensioned solely on the basis of equality of Froude numbers, thus being referred to as "Froude Law" models (Fischer, 1979).

A further complication in modeling large rivers and estuaries arises from the need to distort the vertical scale in relation to the horizontal. The necessity typically arises because the prototype is so large that the horizontal scale must be made relatively small for practical reasons (economy, space, and time available to the modeler). Thus horizontal scales are typically in the range of 1:1000. (Fischer, 1979) If the vertical dimension were set equal to the horizontal, the resulting depth of the fluid in the model would be so small that viscous and surface effects would significantly affect the fluid motion. This is contrary to the assumption previously made that viscous and surface effects are negligible. Additionally, vertical measurements (e.g. tide levels) would be of such small magnitude that accuracy would be impaired. The solution to these problems is to distort the vertical scale; ratios on the order of 1:100 are commonly used. (Fischer, 1979) The increased depth of the fluid in the model both increases the accuracy of measurements and ensures that the flow remains turbulent, thus preventing undesirable viscous effects.

Scale distortion of Froude Law model obviously sacrifices, to some degree, the dynamic similitude between model and prototype. As a result, distorted Froude-scaled models can only simulate Froudian phenomena such as tidal currents or gravitational circulation.

Non-Froudian phenomena such as eddies and local currents may not be accurately represented by the model.

Scale distortion has a significant effect on the rates of vertical and horizontal dispersion and diffusion. This effect has been the subject of numerous studies (Abraham, 1975, Fischer and Holley, 1971, Slotta and Tang, 1976, Fischer et al, 1979). Consider the conservation equation of a conservative tracer (Abraham, 1975):

$$\underset{(1)}{\frac{\partial C}{\partial t}} + \underset{(2)}{U\frac{\partial C}{\partial x}} + \underset{(3)}{V\frac{\partial C}{\partial y}} + \underset{(4)}{W\frac{\partial C}{\partial z}} - \underset{(5)}{\frac{\partial}{\partial x}\left(D_x\frac{\partial C}{\partial x}\right)} - \underset{(6)}{\frac{\partial}{\partial y}\left(D_y\frac{\partial C}{\partial y}\right)} - \underset{(7)}{\frac{\partial}{\partial z}\left(D_z\frac{\partial C}{\partial z}\right)} = 0 \qquad \text{(eq. 7)}$$

where: C = concentration

U, V, W = velocity components in x, y, & z directions

Dx, Dy, Dz = diffusion coefficients in x, y, & z directions

Terms 2, 3, 5, and 6 of equation 7 give;

$$(Dx)_r = (Dy)_r = U_r L_r \qquad \text{(eq. 8)}$$

and terms 4, and 7 give;

$$(D_z)_r = W_r H_r \qquad \text{(eq. 9)}$$

where: H = characteristic vertical length

L = characteristic horizontal length

the subscript r refers to scale ratio, eg. $\frac{LM}{Lp} = Lr$

Three characteristic parameters may be considered which relate eddy velocities and lengths;

$$D \propto U^* H \qquad \text{(eq. 10)}$$

$$D \propto UH \qquad \text{(eq. 11)}$$

$$D \propto UL \qquad \text{(eq. 12)}$$

where U^* = shear velocity = $(\tau o/\rho)$ (a measure of the intensity of the turbulent fluctuations)

Clearly, there is a discrepancy between the ratios expressed in equations 8 and 9 and those given in equations 10, 11, and 12. Table 1 shows the actual scale on which diffusion coefficients are reproduced in a distorted Froudian model divided by the scale ratios required by equations 8 and 9, for each of the characteristic parameters in equations 10, 11 and 12.

TABLE 1 Reproduction of Diffusion in Distorted Froudian Models (Abraham, 1975)

Characteristic Parameters	D(Actual) / D(Required)	
	horizontal	vertical
U^*H	$H_r^{3/2} L_r^{-3/2}$	$H_r^{-1/2} L_r^{1/2}$
UH	$H_r L_r^{-1}$	$H_r^{-1} L_r$
UL	1	$H_r^{-2} L_r^2$

In general, distorted Froudian models tend to overpredict lateral diffusion rates and underpredict vertical diffusion rates. Experimental evidence of this has been provided by Crickmore (1972) in a study of tidal flow in Heysham Harbor, England. In comparing field and model observations of the dispersion of a continuous source of tracer, it was noted that the model plume spread faster transversely and slower vertically than the prototype plume. Crickmore concluded that a model was valuable for showing mean flow paths resulting from tidal oscillation, but that diffusion rates must be estimated using field data.

Thus, a distorted Froude Law model will not precisely reflect the condition of the prototype at any given instant. In many cases, however, (including this study) the information of interest is not the instantaneous behavior of the system. Rather, the study is concerned with circulation and flushing patterns which extend over comparatively long periods of time (e.g. several tidal cycles). Under these criteria, distorted scale models have been shown to provide effective, useful results (Slotta and Tang, 1976).

When using distorted Froude Law models, the following relations can be defined between the vertical, horizontal, velocity, and time scales (ASCE, 1942):

$$T_r = \frac{L_r}{H_r^{1/2}} \qquad \text{(eq. 13)}$$

$$U_r = H_r^{1/2} \qquad \text{(eq. 14)}$$

where T_r = time ratio (model:prototype)

U_r = velocity ratio (model:prototype)

L_r = horizontal length ratio (model:prototype)

H_r = vertical length ratio (model:prototype)

B. Design and Construction of Model

The objective of the model study was to gain an understanding of the circulation patterns and flushing rates in the Port of Astoria. A knowledge of the residence time of water, together with any sediments or pollutants carried with it, in the slips at the Port is necessary to an understanding of the circulation present. Numerous variables affect the circulation in an estuary; basin geometry, tidal volumes, tidal periodicity, fresh water runoff, the physical and chemical differences between the saline and fresh water in the system, and the effects of wind-induced waves and currents (Wright, 1974). Fortunately, the system to be modeled at the Port of Astoria is a comparatively simple one in which several of these variables can be assumed negligible.

Figure 5 shows the area included in the model. Essentially, Slip #1 and Slip #2 were each treated as a small embayment closed on the landward side, and open on the "seaward" side to the Columbia River. Consequently, no fresh water inflow is present, with the result that essentially no stratification due to temperature and salinity variation occurs. As for wind-induced waves and currents, the comparatively small lengths of the estuaries under consideration do not provide sufficient fetch for significant wind-induced motion to develop. Wind-induced phenomena can therefore be assumed negligible except at the very surface.

The horizontal and vertical scales of the model were determined by the available space in the modeling tank, which was 4 ft

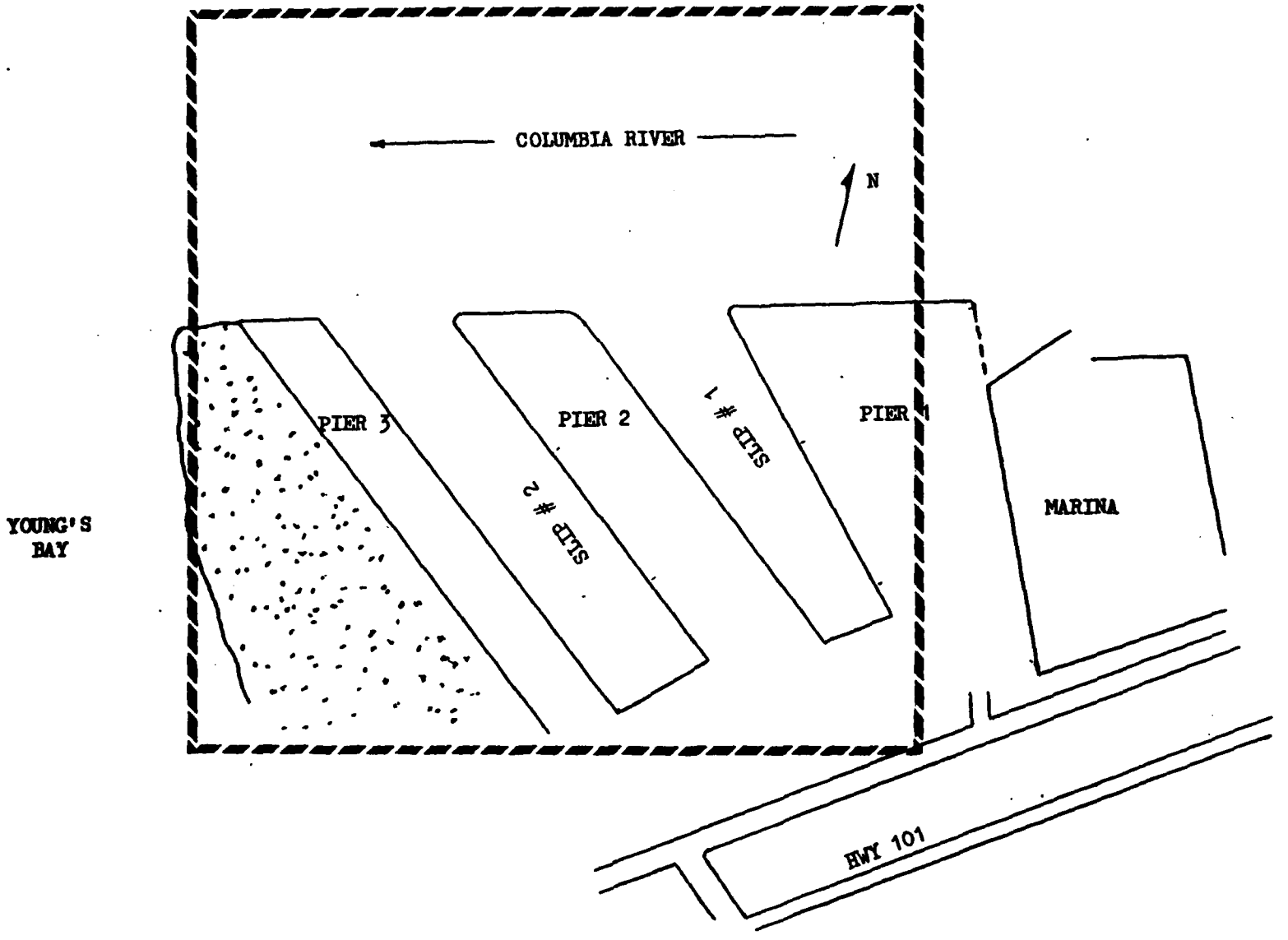

Figure 5 PHYSICAL MODEL, PLAN VIEW

(1.2 m) square, constructed of clear plexiglass. The largest scales which could conveniently be used were 1:1200 horizontally and 1:120 vertically. Since no velocity measurements were to be made, the only remaining scale to be determined was the time ratio, in order to correctly simulate the periodicity of the tide. Using equation 13;

$$T_r = \frac{L_r}{H_r^{1/2}} = \frac{1/1200}{(1/120)^{1/2}} = \frac{1}{109.54} \qquad \text{(eq. 15)}$$

The correct tidal period for the model was determined by scaling the tidal period of the prototype, approximately 12.4 hours.

$$T_{model} = \frac{(12.4 \text{ hr})(60 \text{ min/hr})(60 \text{ sec/min})}{109.54} = 408 \text{ sec} \quad \text{(eq. 16)}$$

or about 6.8 minutes.

The model was constructed of 1/8" (3mm) plastic stock appropriately configured and welded or glued into place. Land areas were covered, either with plastic or cardboard (above the high tide level) to prevent light from showing through. Lights were then installed under the model with a reflector so that the areas representing water were clearly illuminated. A Super-8 movie camera was fixed above the model to record the movement patterns of the dye tracers which were used.

The flow pattern was simulated by the superposition of two pumping systems. One, representing the flow of the Columbia River, consisted of a pump which provided a constant uni-directional (downstream) flow in the model. The second, representing the periodic tidal flow, consisted of a pump and valves which could be used to

generate upstream flow (incoming tide) and reversed to generate downstream flow (outgoing tide). To prevent an excessive amount of dye from accumulating in the model, the water was not recirculated. In spite of this, dye buildup occured fairly rapidly due to the relatively small volume of water in the model. As a result, the system had to be thoroughly drained and flushed quite frequently, usually every 8-10 tidal cycles.

C. Model Application and Results

Since the model was intended to provide only general information concerning the hydraulic exchange within the port area environs, the model tide amplitude was established corresponding to the maximum tide range experienced at Astoria. The hydrodynamic patterns thus determined should apply equally well to lesser tide ranges, (i.e. although actual velocities and accelerations may differ, the flow patterns would be similar).

Approximately forty different tests were run, each consisting basically of the following steps:

a. Activate pumping systems and lights.

b. Introduce the dye tracer into the system where desired. The dye was introduced instantaneously (slug) or continuously (trickle) or by a combination of both methods.

c. Turn on the camera to record the movement patterns of the dye tracer.

d. Run the model for about 6 tidal cycles.

e. Secure the model and camera, drain and flush the model tank of accumulated dye, and prepare for the next run.

A wide variety of locations were selected for dye release.

Both slug and trickle injections were made at frequent intervals along the length of each slip. Additionally, dye tracer releases were made in the river channel; a continuous injection upstream to represent dissolved and/or suspended constituents (e.g. suspended sediments) in the ambient river water, and a slug injection just outside the mouth of each slip, to represent the effect of disposing of dredge spoils at this location.

The prevention of sedimentation is of great concern at the Port of Astoria, a fact which was considered when determining appropriate test conditions. To further investigate this particular problem, the model was modified by the addition of impervious wall sections for a number of runs. The impervious sections represented possible structures (e.g. silt curtains, sheet piling) which might feasibly be constructed at the Port to improve the hydrodynamic patterns as they affect sedimentation. It was surprisingly difficult to so modify the hydrodynamics without resorting to configurations which were unlikely to be practical in reality.

The results from the model were highly illuminating and satisfactory.

Figure 6 shows the results of one of the model runs which clearly illustrated the interaction between the slips. Dye was released continuously in slip #2 as shown. Figure 6(a) gives the motion of the dye on the ebb tide. The dye dispersed in slip #2 and flowed into the Columbia River, whence it proceeded downstream. Figure 6(b) illustrates the changes in flow patterns which occurred during flood tides. As the flow in the Columbia River reversed, the

Figure 6 Dye Movement in Physical Model

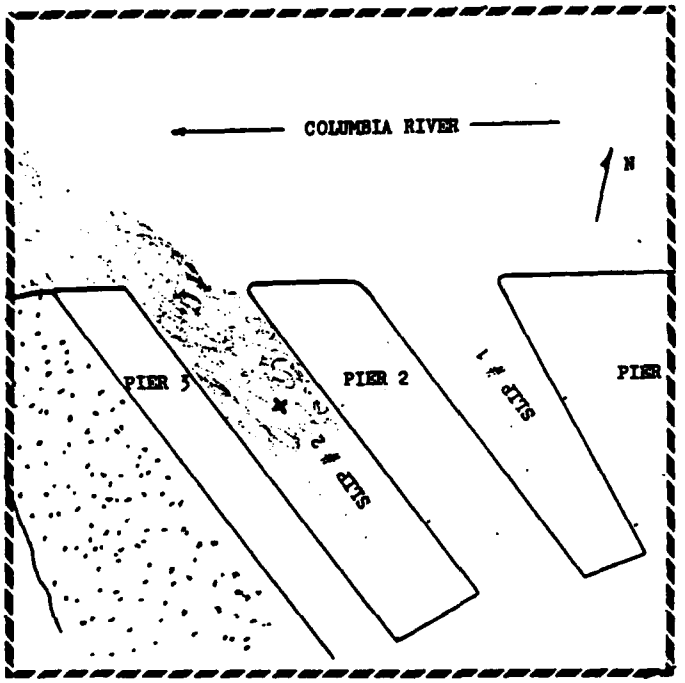

(a) Ebb Tide

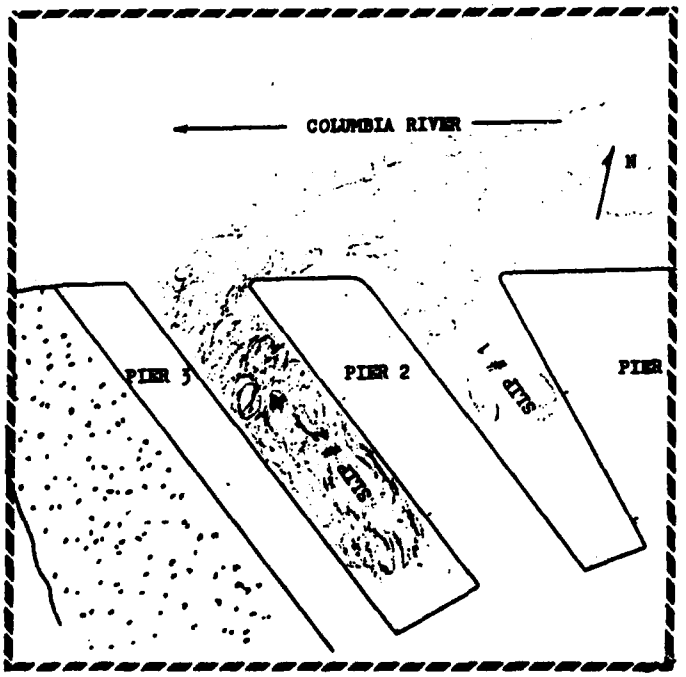

(b) Flood Tide

dye was carried in an upstream direction to and past the mouth of slip #1. A portion of this dye drifted into slip #1 and remained there, even on the next ebb tide. The implication of this behavior for the Port of Astoria is that the generation of large volumes of suspended sediments in one slip (e.g. disposal of dredge spoils in slip #2) can result in increased sedimentation in the other slip. This is of concern at the Port of Astoria, since disposal of dredge spoils into the Columbia River is only permitted during periods of high flow. Consequently, it may at times be necessary to adopt the seemingly contradictory policy of disposing of dredge spoils in one slip to keep the other slip navigable.

The film records were transferred to videotape for presentation to officials at the Port of Astoria. The simplicity and flexibility of the model were particularly attractive features. Test runs could easily be made to simulate virtually any desired conditions in the field, both existing and proposed. Additionally, the simplicity of the model renders the film results easily comprehensible to anyone, familiar or not with hydraulic modeling.

The model results compared favorably with aerial photographs of dye releases in the field. Correspondence between the model and prototype was excellent for a dye release at the Port of Astoria on the incoming tide. Correspondence was less satisfactory for the field dye release made on the outgoing tide, but this probably resulted from the stiff breeze which was blowing against the outgoing tide. Although the wind was assumed only to affect the very surface of the water, this would be sufficient to produce apparent discrepancies in

the aerial photographs (which only record the situation on the surface). A further discussion of the field exercise is given in Section VI.

In summary, a model of this type can be a useful tool in gaining an understanding of the hydraulic exchange of a prototype system. Such a model might be particularly useful as a management tool in performing preliminary investigations into the possible impacts of proposed actions which may affect the prototype.

V. 1-Dimensional Flushing Model

A. Theory

Consider a body of water near a coastline which is subject to tidal fluctuations as shown in fig. 7 (Mc Dougal, 1980).

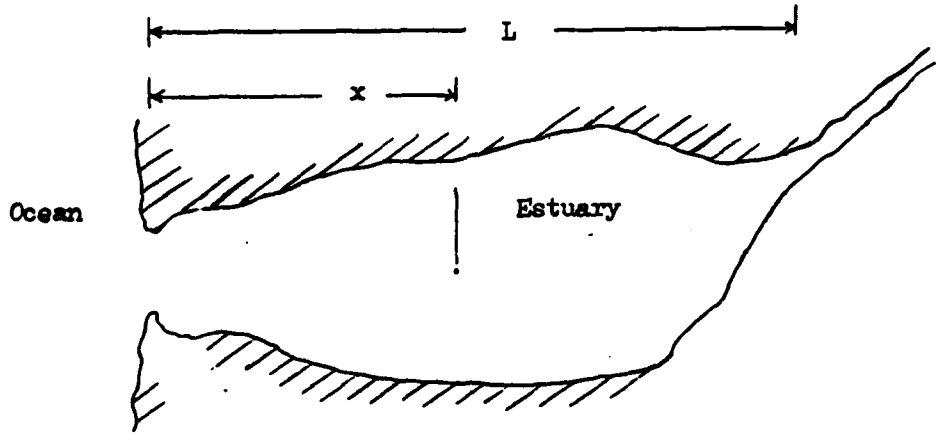

Figure 7

The free surface displacement from the mean water line (MWL) at a point x at time t is:

$$\eta(x,t) = (a) \cos\left(\frac{\omega}{(gh)^{1/2}} x\right) \sin(\omega t) \qquad \text{(eq. 17)}$$

where a = tidal amplitude

ω = tidal frequency

x = distance from mouth

L = overall length from mouth

g = acceleration of gravity = 32.2 ft/s^2 (9.81 m/s^2)

h = still water depth (average)

t = time

Assuming that h is on the order of magnitude of 100 ft (30 m),

$$\frac{\omega}{(gh)^{1/2}} = \frac{.14 \times 10^{-3}}{((32.2)(100))^{1/2}} = 2.5 \times 10^{-6} \qquad \text{(eq. 18)}$$

Then if L is on the order of 10^4 ft (3×10^3 m)

$$\frac{\omega}{(gh)^{1/2}} (L) \approx 10^{-1} \qquad \text{(eq. 19)}$$

and

$$\cos \left(\frac{\omega}{(gh)^{1/2}} L\right) = \cos (10^{-1}) \approx .995 \approx 1.0 \qquad \text{(eq. 20)}$$

equation (17) then becomes

$$\eta(x,t) = \eta(t) = a \sin \omega t \qquad \text{(eq. 21)}$$

Equation (21), in conjunction with conservation of momentum and continuity of flow, were used by Mc Dougal to develop a simple 1-Dimensional numerical model for flushing in relatively narrow estuaries. If the assumption that $\cos \frac{\omega L}{(gh)^{\frac{1}{2}}} \approx 1.0$ is valid, the only values which vary over space are flow rates and concentrations of dissolved or suspended constituents.

B. Numerical Model

Fig. (8) Definition Sketch

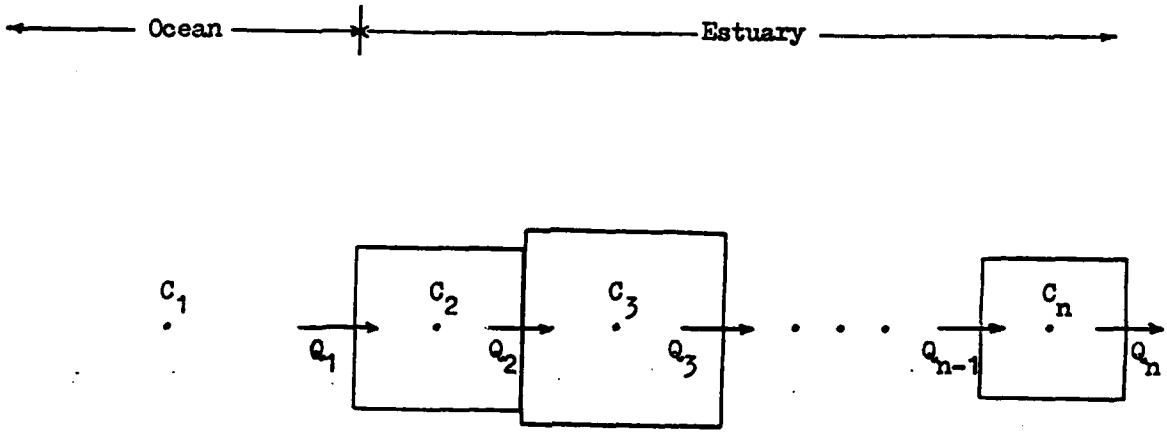

As shown in fig. 8, the flow rates Q_n are defined at the grid boundaries and the concentrations, C_n, are defined at the grid centers. The model has a total of N grids, of which grid #1 always represents the open ocean, or in this case the Columbia River, as a boundary condition.

The flow rates Q_n can be determined from continuity. Let L_n and W_n represent the length and width of grid n. The flow rate Q_n across the interface between grids n and n+1 is the rate change of the volume of water upstream (landward) of the boundary.

$$Q_n(t) = \left(\sum_{i=n+1}^{N} W_i L_i \right) \frac{dh}{dt} \qquad \text{(eq. 22)}$$

from equation 21, $\frac{dh}{dt} = \frac{d\eta(t)}{dt} = \frac{d(a \sin(\omega t))}{dt} = a\omega\cos\omega t$

$$Q_n = \left(\sum_{i=n+1}^{N} W_i L_i \right) a\omega\cos\omega t \qquad \text{(eq. 23)}$$

From conservation of mass, the concentration, C_n, of a (conservative) constituent present in grid n at time $t^{k+1} = t^k + \Delta t$, can be determined.

Consider first an incoming tide:

$$M_n^{k+1} = M_n^k + (\text{mass flowing in from n-1}) - (\text{mass flowing out to n+1}) + (\text{sources/sinks}) \qquad \text{(eq. 24)}$$

Taking $$C_n^k = \frac{M_n^k}{V_n^k} = \frac{M_n^k}{W_m L_n (H_n + \eta(k))} \qquad \text{(eq. 25)}$$

$$M_n^k = C_n^{k+1} V_n^{k+1} = C_n^k (W_n L_n (H_n + \eta(k)) + C_{n-1}^k Q_{n-1}^k \Delta t - C_n^k Q_n^k \Delta t + S \Delta t \qquad \text{(eq. 26)}$$

$$C_n^{k+1} = \left(\frac{1}{W_n L_n (H_n + \eta(k+1))}\right)\left((C_n^k (W_n L_n (H_n + \eta(k))) + (C_{n-1}^k Q_{n-1}^k - C_n^k Q_n^k + S) \Delta t\right) \qquad \text{(eq. 27)}$$

A parallel equation can be derived for the outgoing tide by reversing the signs of the terms involving Q_{n-1} and Q_n.

Finally, the total mass present in any grid can be determined as the product of the concentration and volume in the grid.

The FORTRAN program for the model is given in Appendix B. The program has been written to accomodate a variety of different situations. Any combination of one of the following initial conditions with one of the source configurations can be used.

Initial Conditions:

1) Initial masses (uniform or distributed)

2) Initial concentrations (uniform or distributed)

3) No mass/concentration in estuary but some concentration in ocean.

Source Configurations: (for each cell in the model)

1) No source

2) Finite source

3) Continuous source

Note that the sources could be represented as sinks by using negative values.

C. Application to the Port of Astoria

The 1-dimensional model was applied to Slip #1 (the easternmost slip) at the Port of Astoria. The geometry of the slip is appropriate to the use of the 1-dimensional model in that the slip consititutes a relatively long, narrow "estuary" open to the tide (in the Columbia River) at one end.

1. Grid Scheme: Slip #1 is shown in fig. 9. Two different grid schemes were used, one using six cells, the other having nine cells. In both cases, cell number one represents the Columbia River. The grid dimensions are as shown in Table 2.

Figure 9

SLIP # 1, PORT OF ASTORIA

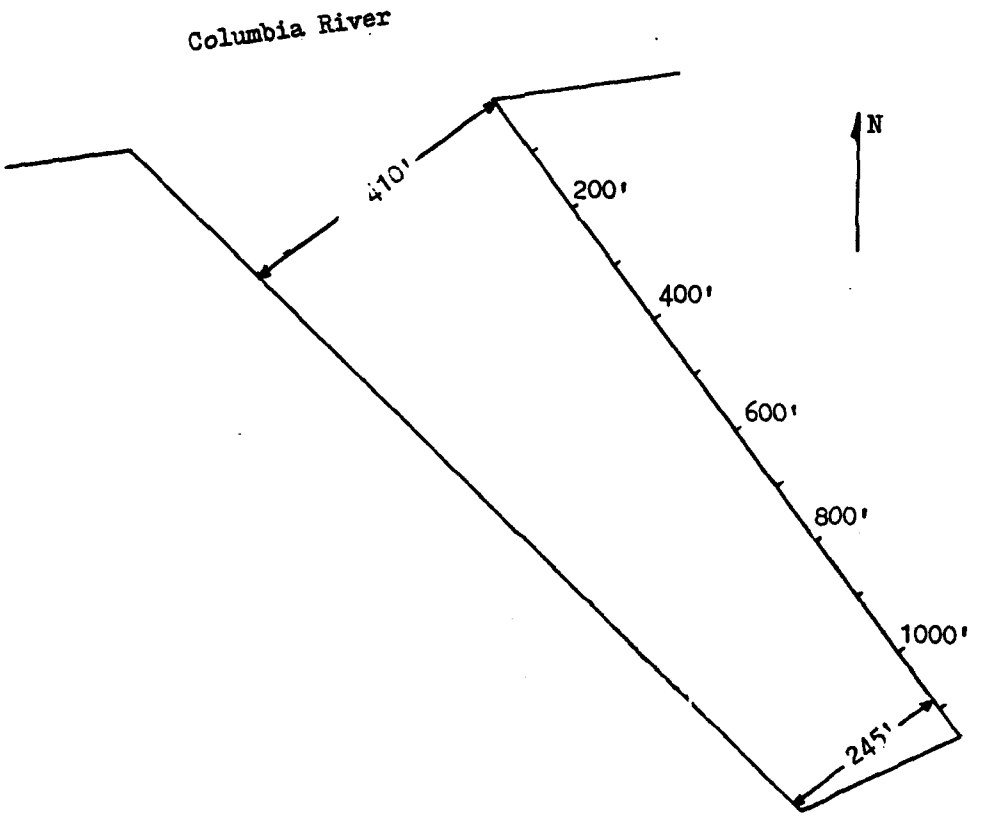

Table 2 Grid Dimensions (ft)

grid number	MODEL 1 Length (L)	Width (W)	Depth (H)	MODEL 2 Length (L)	Width (W)	Depth (H)
1	0	0	0	0	0	. 0
2	200.0	395.0	32.0	100.0	402.5	32.5
3	200.0	375.0	33.0	100.0	387.5	32.0
4	200.0	335.0	32.5	100.0	372.5	33.0
5	200.0	305.0	36.5	100.0	357.5	33.0
6	300.0	267.5	10.0	100.0	342.5	32.5
7	--	--	--	100.0	327.5	33.0
8	--	--	--	200.0	305.0	26.5
9	--	--	--	300.0	267.5	10.0

(Note: 1 ft = .305 m)

Output from the model is presented graphically, using a separate plotting routine. Two types of output plots are used:

1) If a cell has an initial concentration (other than zero) the output may be plotted as relative concentration (percent of the original concentration) versus time.

2) If a cell has an initial concentration of zero, no relative concentration can be computed. In this case, the output is plotted as absolute concentration versus time; with the concentration being in whatever units are specified in the model input.

Figure 10 illustrates the model results for three runs in which initial (normalized) concentrations of 100 were established in the landward (highest numbered) grids of the models. Figures 10(a) and 10(b) show the relative concentration versus time in grids number six of six grid models with tidal amplitudes of 2.0 ft (.61 m) and 5.0 ft (1.72 m) respectively. Figure 10 shows the relative concentration versus time in grid number nine of a nine grid model for a tidal amplitude of 5.0 ft (1.72 m).

The rate of flushing predicted over 100 hours varies among the three models, ranging from 78% to 92%. Given the same number of grids in the model (i.e. for figures (a) and (b)) the higher tidal amplitude results in a greater predicted flushing rate. This is reasonable, since greater tidal amplitudes result in larger exchanges of water between adjacent cells in the model. .A more subtle result is that, given the same tidal amplitude (i.e. figures (b) and (c)) the model with the greater number of cells predicts lower flushing rates. This "numerical retardation " effect is important when numerical models are employed. Basically, as the number of grids in the model increases, the volume exchanged between the grids decreases, which results in an apparently lower rate of hydraulic exchange. Determining the optimum number of grids to be used in the model is an important aspect of model calibration.

Figure 11 illustrates concentration versus time for grids located near the midpoint of the slip (grid #4 or #5) and at the mouth of the slip (grid #2) with tidal amplitude equal to 5.0 ft (1.72 m).

Figure 11 shows the concentration versus time given an

Figure 10

Relative Concentration vs Time

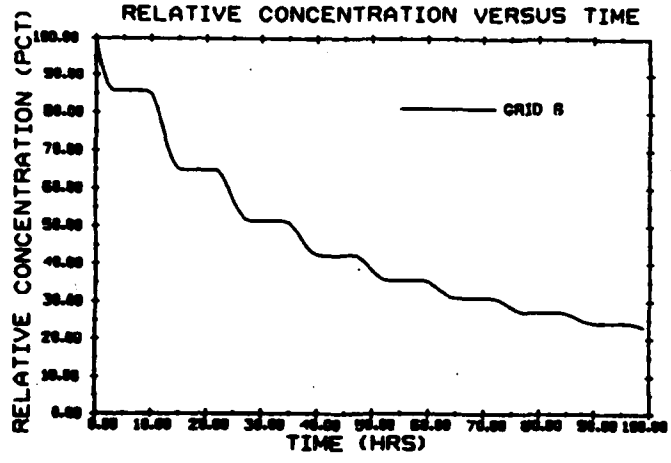

(a)

a = 2.0 ft

$C_{0,6}$ = 100

S = 0

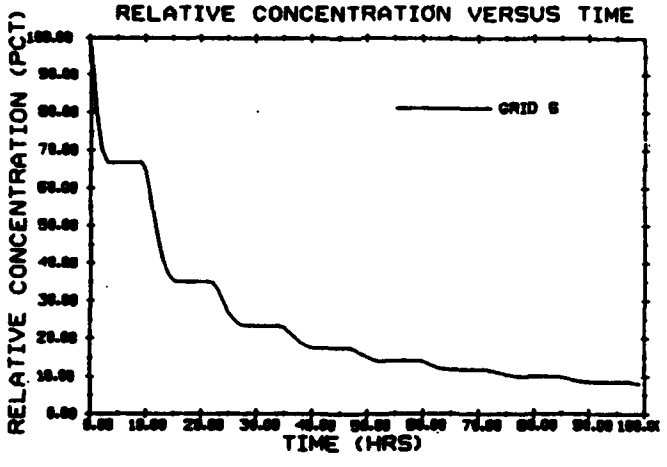

(b)

a = 5.0 ft

$C_{0,6}$ = 100

S = 0

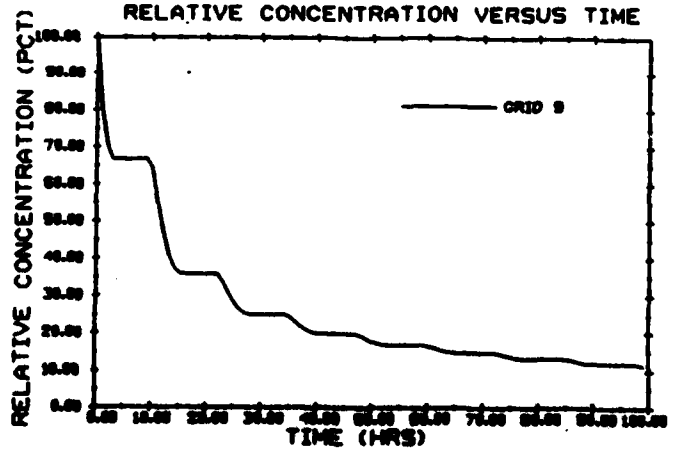

(c)

a = 5.0 ft

$C_{0,9}$ = 100

S = 0

Figure 11

Concentration vs Time

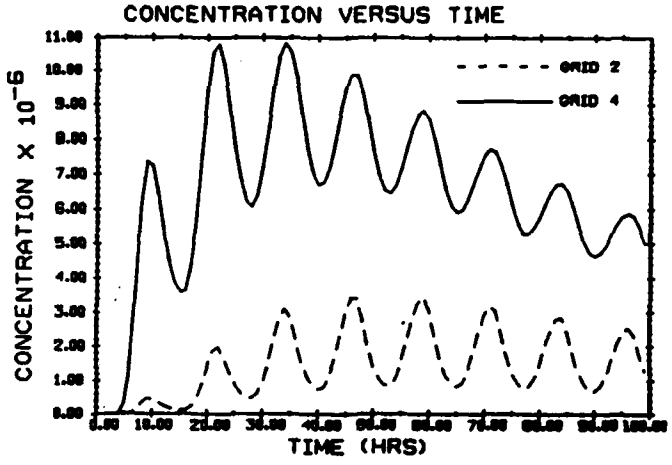

(a)

a = 5.0 ft

$C_{0,6}$ = 100

S = 0

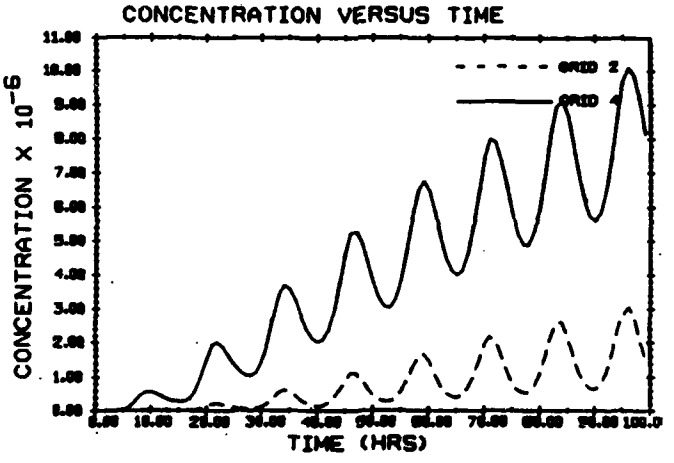

(b)

a = 5.0 ft

C_0 = 0

S_6 = 1

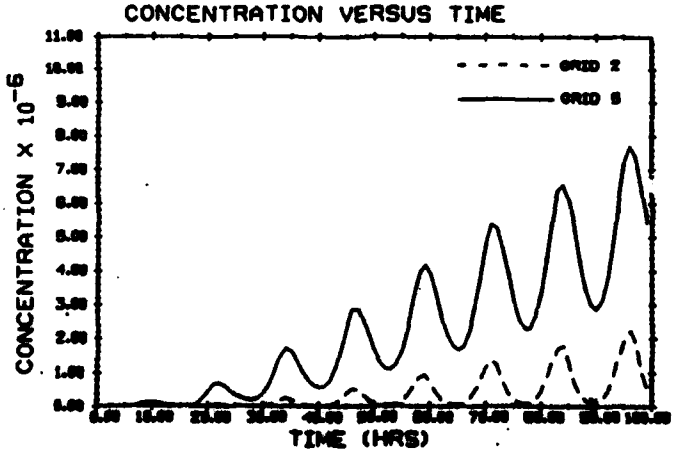

(c)

a = 5.0 ft

C_0 = 0

S_9 = 1

initial concentration of C = 100 units in cell number six of a six cell model. The resultant concentrations in grids #2 and #4 begin at zero, rise to a peak, then decrease at a declining rate, which would eventually become asymptotic to C = 0. Note that the concentration in grid #4 reaches its maximum in about half the time (25 hours as opposed to 45 hours) that grid #2 requires. Also, the maximum concentration in grid #4 is about three times the maximum attained in grid #2.

Figure 11 shows the concentration versus time given no initial concentration anywhere in the slip, but with a constant input of one unit per hour into grid #6 of a six grid model. The resultant concentrations in this case begin at zero and increase at a decreasing rate. Eventually, the concentrations would level out as the system attained its steady-state.

Figure 11 shows the concentration versus time given an initial condition of zero concentration throughout the slip and a constant input of one unit per hour in cell nine of a nine cell model. The resultant concentration plots are similar to those in figure 11, but again the effect of numerical retardation is evident. Both of the models reflected in (b) and (c) will eventually reach the same steady-state concentrations. Due to numerical retardation, however, the nine grid model will approach the steady-state more slowly.

The model results give an indication of the hydraulic exchange which occurs between slip #1 and the Columbia River. The predicted flushing rates (80%-90% over four days) indicate that the slip exchanges sufficient water to avoid stagnation. Another

inference which may be drawn is that sufficient suspended sediment-laden water from the river enters the slip to provide the source of the shoaling which occurs there. Further, the numerical circulation model's estimated residual concentrations may be used as a first-cut for the purpose of planning field studies. Finally, the numerical circulation model estimates the flow rates into and out of each cell over time. From these flow rates, the average velocity of the water flowing in the slip may be approximated, which velocities may be important when considering the process of sedimentation which occurs within the slip.

Based on the model results, a field study was planned to calibrate the model. It was intended to release Rhodamine WT into the landward end of Slip #1 and monitor the concentration over time in the slip using a fluorometer. The calculations involved in determining the required quantities of dye to be released are shown in Appendix B. The basic consideration is to release the minimum amount of dye necessary to obtain residual concentrations in a range which can be accurately measured by the fluorometer.

Unfortunately, due to a combination of factors including equipment problems, the author's inexperience, and a heavy workload at the Port, useable quantitative data was not obtained from the dye tracer experiment in the field. (A further discussion of the field study is provided in Section VI.) As such, the model remains uncalibrated. Thus, while it may provide useful insights into the qualitative aspects of the circulation patterns at the Port, further field data is needed to calibrate the model before it can be considered quantitatively reliable at Astoria.

VI. Numerical Sedimentation Model

A. Theory

The source of the sediment which accumulates in the Port of Astoria is evidently the suspended load carried by the water in the Columbia River which enters the slips during each incoming tide (it is not, however, entirely clear whether the sediments originate upstream in the Columbia or whether their origin is the Young's River). As a result of the low current velocities present in the slips, compared to the current velocities in the channel, a certain proportion of the suspended sediment settles out of the water onto the floor of the slip and is left behind when the water flows out of the slip on the ebb tide. Also, as a result of the low current velocities in the area, bedload transport of sediment may be assumed to be negligible.

In an attempt to estimate the rate of accumulation of sediment in the slips, a numerical sedimentation model has been developed. Consider a semienclosed harbor open to a tidal estuary, as illustrated in figure 12.

Figure 12. Typical Semienclosed Harbor

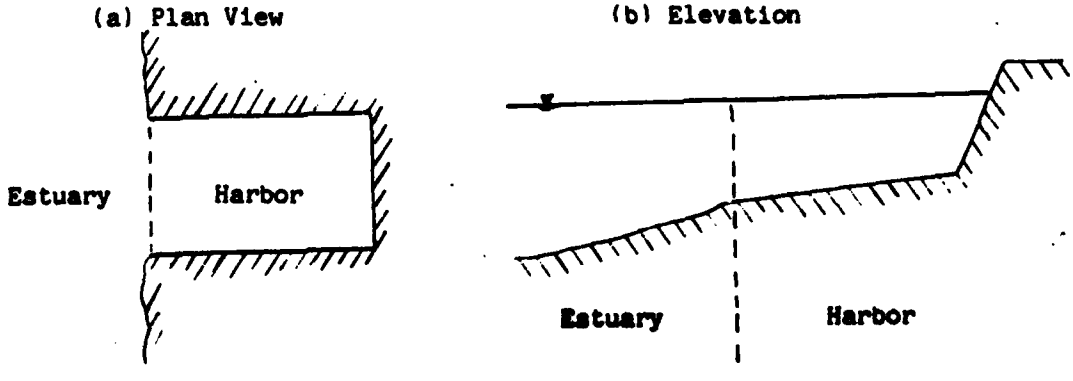

If the length of the harbor is assumed to be small compared to the length of the tidal wave, equation 21 may be applied to determine the displacement of the water surface from the mean water level.

$$\eta(x,t) = \eta(t) = a \sin \omega t \qquad \text{(eq. 21)}$$

By making the following additonal assumptions, Everts (1981) developed a mathematical model in integral form for the prediction of sedimentation rates in semienclosed harbors.

(a) sediment enters the basin in suspension.

(b) Bedload sediment transport is negligible (i.e., once sediment is deposited it's no longer subject to movement)

(c) Water enters or leaves the harbor as the water surface rises or falls in the adjoining estuary.

(d) At any point in time, the flow into/out of the harbor will be uni-directional or non-existent.

(e) Shoaling and sedimentation processes occur uniformly throughout the harbor area.

Based on the available data and field observations, these assumptions appear to be reasonable for the Port of Astoria.

Everts (1981) presents analytical solutions for a number of situations in which the model may be employed. Based on the concepts and assumptions used by Everts, a single cell, finite element model has been developed for estimating sedimentation rates at the Port of Astoria.

Figure 13 is a definition sketch for the model.

Figure 13 Definition Sketch

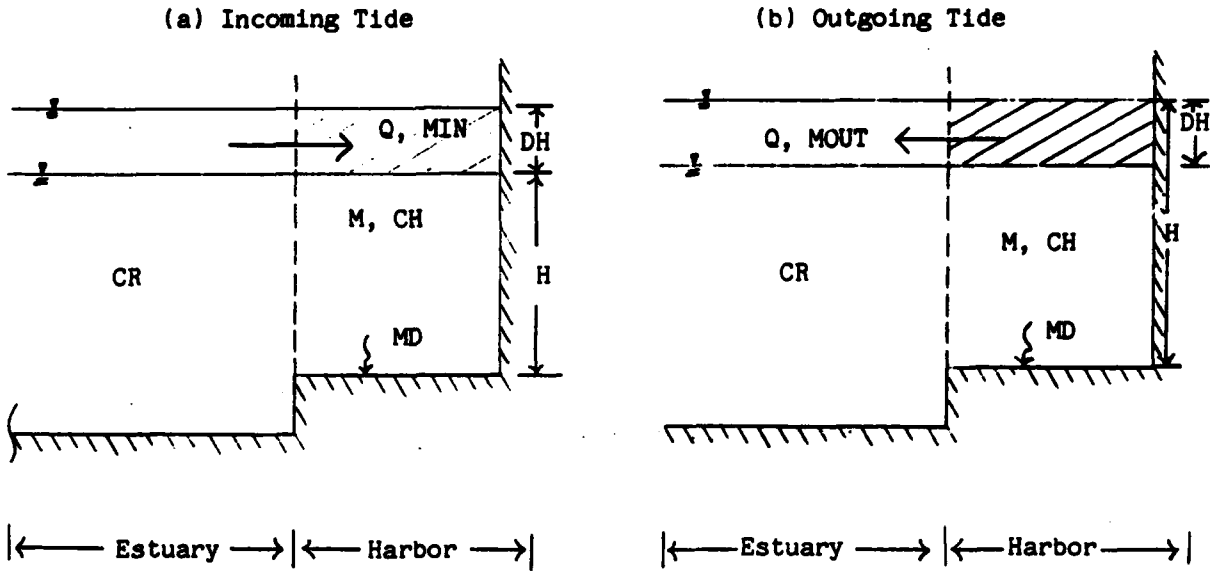

CH = Average concentration of suspended sediment in the harbor

CR = Average concentration of suspended sediment in the river

M = Mass of suspended sediment present in the harbor

MIN = Mass of suspended sediment which flows into the harbor during time increment DT

MOUT= Mass of suspended sediment which flows out of the harbor during time increment DT

Q = Volume of water flowing in or out of the harbor during the time increment DT

DH = Change in water surface level during DT

MD = Mass of sediment deposited on the bottom of the harbor

DT = Time increment

H = Depth of water in the harbor (average).

(Note: In accordance with assumption (d), either MIN or MORT or both must be zero at any given time.)

Additonal variables may be defined as follows:

A = Plan area of the harbor

VS = Settling velocity of the sediment

MV = Mass of sediment per unit volume of deposition

By conservation of mass, the mass of sediment present in the harbor at time T + DT may be determined as follows:

$$M(T+DT) = M(T) + MIN - MOUT - MD \qquad \text{(eq. 28)}$$

(1) (2) (3) (4) (5)

Taking Q to be positive for water flowing into the harbor, terms (3) and (4) of eq. 28 may be evaluated as follows:

$$\text{If } Q \geq 0,\ MIN = (Q)(CR)\ ;\ MOUT = 0 \qquad \text{(eq. 29)}$$

$$\text{If } Q < 0,\ MOUT = (Q)(CH)\ ;\ MIN = 0 \qquad \text{(eq. 30)}$$

Evaluation of term (5) of equation 28 requires further data or assumptions concerning the behavior of the sediment in settling, and the concentration distribution of suspended sediment over depth. If you assume that the sediment settles continuously at its settling velocity (VS) over the time increment (DT) without being tossed upward by turbulence, then the individual sediment particles will settle a distance, D, during the period DT, where D is given by

$$D = (VS)(DT) \qquad \text{(eq. 31)}$$

Consequently, all of the sediment within distance D from the bottom of the harbor will be deposited. The mass of this deposition per unit area, MD, is given by

$$MD' = \int_{y=0}^{y=D} C(y)\,dy \qquad \text{(eq. 32)}$$

where:

y = vertical dimension measured upward from the bottom of the harbor; and

C(y) = concentration distribution of suspended sediment.

Figure 14 illustrates this for several possible concentration distributions.

Figure 14 Examples of Suspended Sediment Concentrations

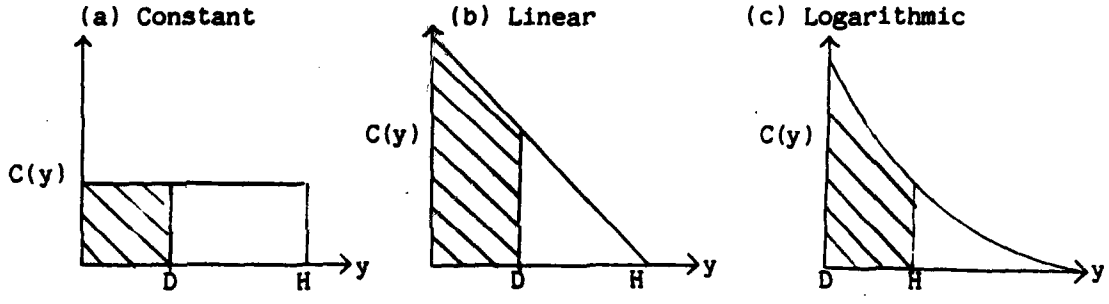

In each case, the sediment concentration must go to zero when y = H, since no suspended sediment can exist above the water surface. The shaded areas represent the mass of sediment deposited per unit area as given by equation 32.

Once the initial mass present in the harbor is established, equation 28 may be applied to any continuous series of time increments. The concentration in the harbor, CH, may also be determined continuously since;

$$CH = \text{Mass/Volume} = (M)/(H)(A) \qquad \text{(eq. 33)}$$

The total mass deposited during time interval DT may be defined as MD and determined by multiplying the mass deposition per unit area by the plan area of the harbor.

$$MD = (MD')(A) \qquad \text{(eq. 34)}$$

The total volume of deposition is given by

$$VOLDEP = MD/MV \qquad \text{(eq. 35)}$$

Since the deposition is assumed to occur evenly over the harbor, the depth of shoaling may be expressed as

$$DSHOAL = (VOLDEP)/(A) \qquad \text{(eq. 36)}$$

Note that at this point the model is quite general in nature. The sediment concentration in the river, which serves as a boundary condition, may vary freely with time, the sediment distribution over depth in the harbor may take on any desired form, and the plan area of the harbor may vary with depth. Furthermore, the equations for the model may be applied to a number of size fractions of sediment, each size fraction having its own settling velocity and concentration distribution. The total sediment deposition in ths case would simply be the sum of the deposits for each of the size fractions. (The use of size fractions is particularly appropriate if there exists a wide range of sizes among the sediment grains, since this may result in widely varying settling velocities and concentration profiles.)

B. Application to the Port of Astoria

The numerical sedimentation model was applied to slip #1 at the Port of Astoria. The sediment characteristics (concentration, grain size, specific gravity, and porosity) were estimated based on field data obtained during the period 24 March 1982 through 24 June 1982. The sediment settling velocities were estimated as a function of the grain diameter using the methods presented in Bogardi (1974). The dimensions of the slip were taken from the data presented in Seciton V for the numerical circulation model.

As the data regarding sediment grain-size was rather limited, a single size fraction, based on the median grain diameter, was used in the model. Considering the relatively small grain sizes present ($D50 \simeq .015$ mm) the vertical distribution of sediment concentration was assumed constant (i.e. as illustrated in figure 14(a)). The plan area of the slip was assumed constant.

The FORTRAN program for the numerical sedimentation model is reproduced in Appendix C, together with the values of the input parameters used in the three model runs discussed in this paper.

Figures 15 (a), (b) and (c) illustrate the results obtained from three model runs with different input parameters. (In the following discussion, the runs will be referred to as (1), (2) and (3) corresponding respectively to figures 15 (a), (b) and (c).

Run (1) was made using the best data available from the field

Figure 15

Depth of Shoaling vs Time

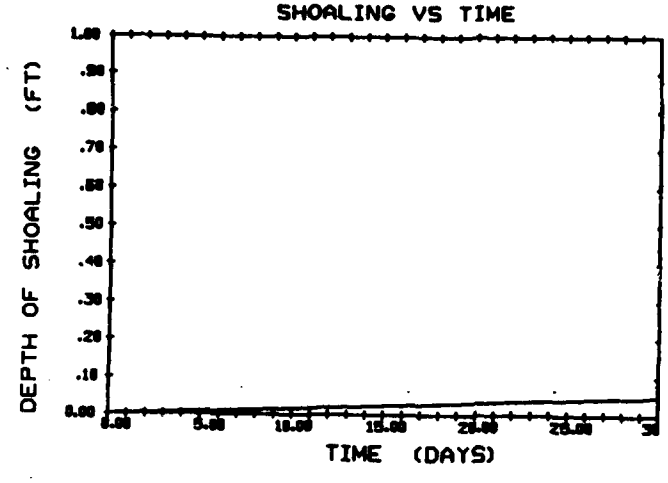

(a)

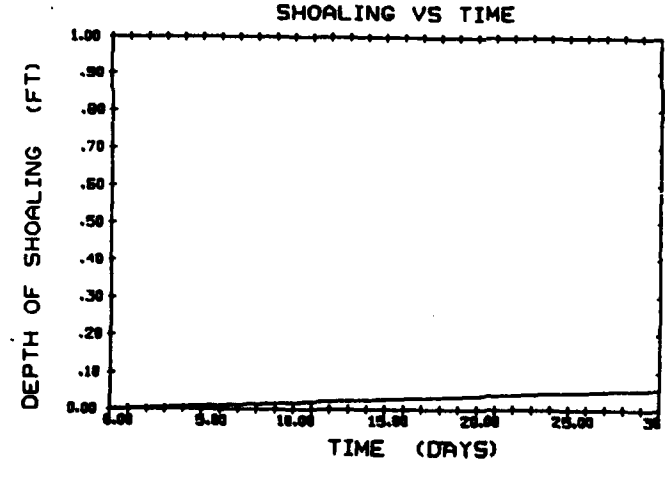

(b)

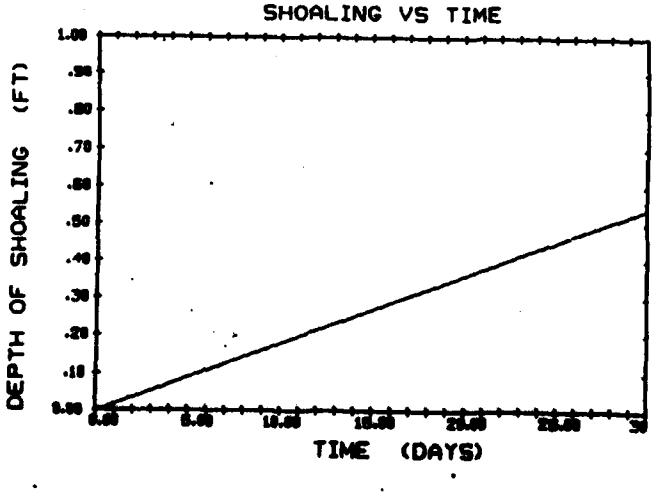

(c)

studies. The model estimated a sedimentation rate of about 0.05 ft/month (.0015 m/month), equivalent to about 0.6 ft/year (.18 m/year). This appears to be approximately an order of magnitude low when compared with actual sedimentation rates experienced at the Port of Astoria.

Two of the input variables are particularly important in determining the models behavior; the concentrations in the Columbia River (CH(N)) and the settling velocities of the sediments (VS(N)). (The initial oncentrations in the harbor are less important, since over a period of time any inaccuracies here will be filtered out by the mass in/mass out iterations.) Unfortunately, both of these variables can only be very roughly estimated given the available data.

Although accurate values for these variables cannot presently be arrived at, their effect on the model can be analyzed by arbitrarily varying the inputs and observing the model response. Runs (2) and (3) were made for this purpose.

For run (2), all input variables were left equal to those in run (1) except that the settling velocity was doubled. As shown in figure 15(b), the doubling of the settling velocity had only a very slight effect on the predicted rate of shoaling.

For run (3), the parameters were left equal to those in run (2) except that the concentration in the Columbia River was increased by a factor of ten. As shown in figure 15(c), this resulted in an almost order of magnitude increase in the predicted shoaling rate. The predicted rate of shoaling in this case was equivalent to about 6.0 ft

(1.8 m) annually, which appears to be consistent with the actual historical rate of sedimentation as estimated by the port officials.

Clearly then, the model is more sensitive to changes in the input concentrations than to changes in the settling velocities of the sediment particles. This result does not appear incompatible with the prototype, where the rate of sedimentation has been observed to vary with the rate of flow of the Columbia River (and hence, with the suspended sediment concentrations in the river). During the winter and spring freshets, for example, the flow rate, the concentration of suspended sediments in the river, and the sedimentation rate in the Port of Astoria have all been observed to increase.

Further research concerning the suspended sediment concentrations in the water entering the slip should therefore be accorded first priority in the further validation and/or refinement of this model. An aspect which should be addressed is the variation over time of these suspended concentrations.

Further research efforts in the area of settling velocities would also be useful. However, due to the relative insensitivity of the model to differences in settling velocities, this information is less critical than the suspended sediment concentrations.

VII. Field Studies

A field exercise was conducted during 17-19 August 1982 at the Port of Astoria. The objective of the study was to collect data which could be used to verify/calibrate the theoretical models which have previously been discussed. The major elements of the field study consisted of dye releases (using Rhodamine WT), aerial photography of the resulting dye patches, and quantitative measurements of dye motion and dilution using a fluorometer. Additionally, current meters were deployed to obtain additional data to supplement previous velocity measurements. Finally, numerous sediment samples were taken from the Port of Astoria and as far west as Young's Bay, to assist in an investigation of the characteristics of the bottom sediments. The activities which related primarily to this paper were the fluorometer test and aerial photography.

A. Fluorometer Test

Fluorometric analysis consists essentially of the introduction of a fluorescent dye into the body of water of interest, and measurement of the resulting dye concentrations with a fluorometer. A variety of techniques can be used for the test. The dye may be released continuously (trickle injection) or instantaneously (slug injection). Likewise, sampling may be instantaneous (grab samples) or continuous (flow-through). Whichever methods are employed, the relative fluorescence of the tracer (before

injection into the water body) and the sample may be used to determine the rate of flow between the point of release and the sampling station (Turner Designs Monograph, 1975).

A number of factors should be considered when selecting a dye for tracer studies (Smart and Laidlaw, 1977, Yotsukura and Kilpatrick, 1973). Sensitivity, detectability, interaction with water chemistry, photochemical and biological decay rates, absorption losses, toxicity, and cost must all be evaluated. In addition, of course, availability must be considered.

Based on the above factors, Rhodamine WT was selected as the dye to be used for the test at Astoria. This dye has been shown to be the preferable tracer for most applications (Turner Designs Monograph, 1975, Smart and Laidlaw, 1977).

The fluorometer used in the test was a Turner Designs Model 10, equipped with a flow-through cuvette for continuous sampling. A Turner Model III fluorometer was previously considered, but was not used due to unstable readings and difficulty with its calibration in the laboratory.

The intended procedure for the fluorometer test was as follows:

1. Release the Rhodamine WT into the landward end of Slip #1 (see Appendix B for calculation of the required quantity of dye) at high tide slack water.

2. Set up the fluorometer near the mouth of Slip #1 and take a continuous sample over the outgoing tide, using a strip-chart

recorder to obtain continuous data.

3. Based on the relative concentrations at the release point and at the fluorometer, calculate the flow in the slip over the 1/2 tidal cycle duration of the test.

The calculated flow rates could then be used to verify the flushing rates predicted by the numerical circulation model described in Section IV.

"The best laid schemes of mice and men gang oft a-gley" (Burns, 1785). This applies particularly to field studies. The level of activity at the Port was particularly high during the period of the field study, which in effect severely hampered these research efforts. For example, it was impossible to set up the fluorometer in the desired location near the mouth of the slip for continuous monitoring due to ship movements. It was therefore necessary to adopt a different approach; the fluorometer was put on board a boat, which was then shifted to different sampling locations in the slip.

Equipment problems presented further difficulties. The strip-chart recorder for the fluorometer failed, which meant that continuous data could not be obtained. Instead, visual observation and manual recording were necessary.

Finally, the dye release was delayed until 5:30 PM (high tide occurred at 2:17 PM) and port operations forced the test to secure at 6:45 PM.

In hindsight, it is perhaps not surprising that the results obtained were sketchy. No discernible pattern of relative

fluorescence could be attributed to the sample results. A possible reason for this is the excessive length of hose attached to the input of the fluorometer. The hose was about 50 feet long, which was appropriate for the intended application of the fluorometer (i.e., if the fluorometer were set on the dock, the hose would have to run some distance on the dock, then over the side and about 30-35 feet down). Also, if the fluorometer were in a continuous sampling/recording mode, the hose length would be relatively insignificant, as it would at most cause a slight time-shift in the fluorescence readings. As the fluorometer was actually used, however, the length of the hose took on a greater significance. The actual sampling method employed was to anchor the boat at various locations, then sample at two foot depth intervals at each location. For this to have produced accurate results, it would have been necessary to allow sufficient time prior to each reading for the volume of water in the hose to be completely displaced, thus ensuring that the sample from the given location and depth would not be contaminated by water from previous sampling locations. In retrospect, and considering the data, insufficient time was probably allowed between samples for the hose to be completely flushed. A preferable solution would have been to replace the existing hose with a much shorter one, which would have been more suitable for use on the boat, and which would have required considerably less time for flushing between samples (the time required is proportional to the volume of water contained in the hose, hence it is proportional to the length of the hose, given that the diameter is constant).

In spite of (perhaps because of) the difficulties encountered and conspicuous lack of success of the fluorometer test, it was a highly instructive experience for the author. In particular, the test brought home the necessity for careful planning prior to field work, including a dry run if possible to gain experience with the equipment. For example, provision of an extra 15 foot length of hose would have been simple if the need had been anticipated. Problems with power supply (12 volt on board the boat versus 120 volt ashore) also might have been anticipated and forestalled by providing an additional transformer. Greater familiarity with the procedures and methods followed by the Port of Astoria might have revealed that various locations in the Port would be off-limits, as far as research, during periods of activity. Overall, the original plan for the fluorometer test lacked the flexibility to cope with these "changed site conditions". The lesson learned is that, in the absence of more thorough and definitive advance knowledge of the conditions which will be encountered, flexibility is highly desirable when planning field studies.

B. Aerial Photography

The second major element of the field exercise was aerial photography of Rhodamine WT dye releases in the slips at the Port of Astoria, and in the Columbia River just off the Port.

Aerial photography can be used to accurately estimate the hydrodynamics of complex fluid systems (Burgess and James, 1971). In

some cases, aerial photography can be analyzed using photogrammetric techniques and computer enhancement of the visual images to estimate mixing coefficients with considerable precision.

The approach in this study was more limited. The primary objective was to release dye on the incoming and outgoing tides, and obtain a time-series of aerial photographs of the movement of the dye patches. This information could then be compared with the result of the physical model.

The equipment used for the aerial photography consisted of two Hasselblad Model ELM cameras with 80 mm lenses. Two different types of 70 mm Kodak film were used, VPS ASA 125 (color print) and Ektachrome 2443 ASA 50 (false color prints). The pictures were taken from a Cessna 150 aircraft from an elevation of about 2000 feet. (It was also intended to use a third camera with infra-red film, but the camera developed mechanical problems in the field and could not be used.)

The first dye release occurred at 10:30 AM on the incoming tide. Dye was released along the centerline of Slip #2 and in the Columbia River to the west (downstream) of the slip. Figure 16 shows the dye release in Slip #2.

A series of aerial photographs were subsequently taken at intervals of 15 minutes for a period of about two hours following the dye release. The false color prints proved to be of limited value, as the dye was scarcely distinquishable in the photographs. The series of color prints, however, provided excellent results, as the dye releases showed very clearly. The pattern of motion was as predicted

Figure 16

DYE RELEASE IN SLIP #2, INCOMING TIDE

by the physical model for an incoming tide; the dye in the slip drifted slowly to the landward end, and gradually dispersed there, while the dye in the river drifted upstream and into the slips, closely reflecting the behavior of similar releases in the physical model. This phase of the aerial photography, then, was quite successful, and tended to confirm the behavior of the physical model.

The second phase of the aerial photography was scheduled for the outgoing tide. A continuous dye release commenced at 3:30 PM from the harbor dredge, moored roughly at the midpoint of Slip #2. Again, a sequence of aerial photographs were taken at 15 minute intervals over two hours. The results, however, were dramatically inferior to those in the earlier sequence. In the second sequence, the dye was barely visible, even in the immediate vicinity of the release point. The water surface appeared extremely dark, essentially obscuring all detail. Consequently, this sequence of pictures was of little value in terms of gaining information on the hydraulic exchange in the port area.

The poor quality of the aerial photographs from the second series was due most likely to the lateness of the hour. As discussed in Burgess and James (1971), the quality of aerial photography is greatly affected by the angle at which the sun's rays strike the water surface. Near mid-day, the light rays strike the water at a steep angle, with the result that some penetration into the water occurs, and the reflected light rays are directed toward an overhead observer. Early or late in the day, however, the incident light rays strike the water surface at a shallow angle, resulting in little or no

penetration. Also, at these hours the reflected light rays leave the surface at a correspondingly shallow angle, comparatively few thus reaching an overhead observer. Judging by the results in this study, this phenomenon indeed has a profound effect on the quality of aerial photography. The ideal solution, therefore, would be to schedule all aerial photography between, say, 10:00 AM and 2:00 PM. Unfortunately, this is not always feasible, due to tidal conditions, operating schedules, etc.

Although the aerial photographs of the outgoing tidal cycle provided little useful data, some interesting information was gained from the exercise. The plane crew (pilot and photographer) observed that the dye tended to drift along the center line toward the rear of the slip. Upon reaching the landward end, the dye spread across the full width of the slip, then drifted along the sides of the slip in the opposite direction; i.e. toward the mouth. The flow pattern on the surface of the slip thus resembled two large eddies, one circling clockwise, and the other circling counter-clockwise, (see fig. 17) a result utterly dissimilar to that predicted by the physical circulation model.

This rather unconventional pattern of flow was evidently the result of wind action. A 10-15 knot wind had been blowing for about eight hours prior to the commencement of the dye release. The wind was from the Northwest, that is, nearly parallel to the long axis of the slip. During most of the day, extensive log rafts were lining both sides of the slip, in position to be loaded aboard ships. As a result, the water surface along the sides of the slip was scarcely

Figure 17

DYE MOVEMENT IN SLIP #1, OUTGOING TIDE

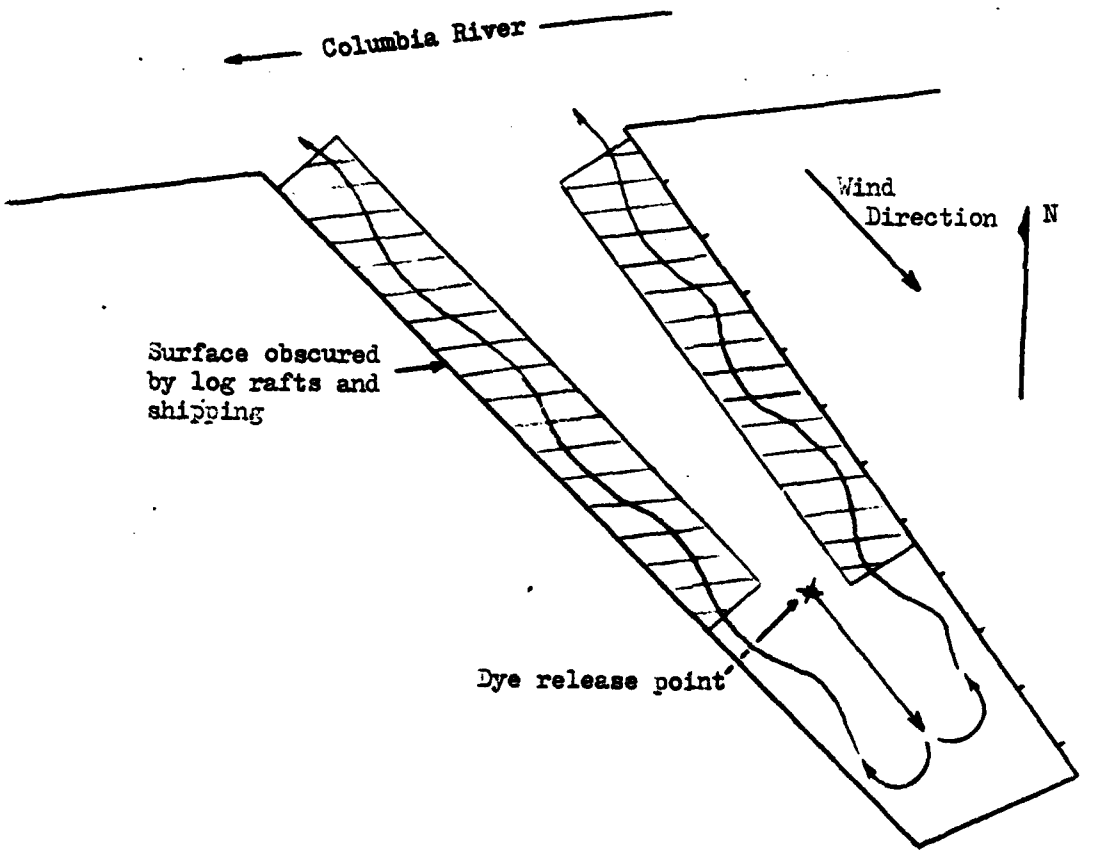

exposed to the wind, whereas the water surface along the centerline was fully exposed. The resultant shear stress of the wind acting on the open water in the center of the slip caused a surficial current to be established toward the rear (landward) end of the slip, even on the outgoing tide. By continuity, the water building up in the landward end of the slip had to go somewhere, hence the outward currents being established along the sides of the slip.

The failure of the observed flow pattern to coincide with the physical model results is not surprising, since wind effects were assumed to be negligible in the model. It would be instructive to repeat the exercise on a windless day (unlikely in Astoria) or with the wind blowing across, rather than along the slip.

The aerial photography represented a considerable expenditure of resources on this project. The results provided some very useful information, particularly the first sequence of pictures illustrating the incoming tide. Scheduling the evolution for the outgoing tide in the late afternoon was a calculated risk. However, given the time and dollars available to the project it was unlikely that further field studies would be possible. Given this constraint, and the state of the tide it was "now or never" to catch an outgoing tide.

A final problem observed in regard to the dye, was that it tended to sink fairly rapidly. This was especially notable during the afternoon release. The sinking of the dye is undesirable in field studies, as it indicates that the specific gravity of the dye is greater than that of the water. As a result, the dye will tend to

settle to the bottom (or possibly some intermediate depth if the water column is highly stratified) and remain there. This effectively defeats the purpose of aerial photography, and may also result in inaccurate results when using a fluorometer. A possible solution to the problem is to dilute the tracer, prior to injection into the water body. If this is done, however, samples of the diluted tracer must be take to determine its fluorescence if a fluorometer test is to be done. Another solution is to inject the dye into a turbulent area, such as near the propeller of a ship, which will cause rapid dilution of the dye. This method was used in the morning releases and appeared to be quite effective.

As a general summary of the field study, it was highly instructive in regard to the problems which can be encountered in this type of work. The problems encountered with equipment vividly illustrated the need for proper maintenance in the shop, as well as the desirability of redundancy in field equipment where possible. Another point that was illustrated with forceful clarity was the need to allow contingency time and avoid scheduling too many activities for too short a time period. Prior experience with the equipment to be employed is also highly desirable in field studies. The last-minute change of fluorometers in this case made the operation in the field slower, more difficult, and probably less accurate than might otherwise have been the case.

A positive aspect of the field exercise was the degree of cooperation with the port officials. In spite of the busy operating schedule (which hindered the field work) the port officials were highly cooperative, to the extent of providing shop facilities and assistance.

VIII. Summary

This paper has presented three models which were used to study the circulation and shoaling characteristics at the Port of Astoria.

The physical model proved useful for gaining an understanding of the overall patterns of circulation in the port area. The nature of the hydraulic exchange between the harbor slips and the Columbia River over incoming and outgoing tidal cycles was clearly illustrated. This information may be of use in analyzing and formulating policies for the maintenance and operation of the Port. For example, the model illustrates the futility of disposing of dredge spoil in the Columbia River unless tides are taken into account. For instance, if the spoil is disposed of in the river to the northwest of the port, a sizeable proportion of the sediment will be washed back into the harbor slips on the incoming tide. A possible solution in this case would be to dredge only at high-water slack and on outgoing tides.

A further potential use of the physical model is for investigating the effect of proposed construction in the port. The model could be easily adapted to simulate the addition of various structures in the port environs, and the resulting changes in the flow patterns observed.

The numerical circulation model provides useful information concerning the hydraulic exchange between the harbor slips and the Columbia River, the mean residence time of water in the slips, and the flushing rate in the slips resulting from tidal fluctuations. In general, one may conclude that the flushing rate in the slips is adequate to prevent stagnant water conditions from occurring; for

average tidal fluctuations, the model predicts about 90% flushing over eight tidal cycles (about four days) at the landward end of the slips. Another useful result of this model is to provide a basis for for the research work in the field. In particular, dye studies would seem to be a useful approach in collecting more data concerning the velocities, diffusion coefficients, and flushing rates actually occuring at the Port of Astoria. This informaton would serve to calibrate the numerical model, so that greater reliance could be placed on it as a tool for predicting future hydraulic phenomena at the port. Finally, of course, the numerical circulation model results serve as the inputs to the numerical sedimentation model.

The numerical sedimentation model provided a reasonable estimate of the sedimentation rate at the Port of Astoria. Further refinement of this model could prove extremely useful. In particular, the effects of varying suspended sediment concentration profiles and time-varying suspended sediment concentrations in the Columbia River are worthy of attention. Further field studies are indicated in these regards. However, if these parameters could be accurately established, then estimates of near-term furture sedimentation rates could be made, possibly allowing more efficient management of dredging operations.

The paucity of accurate field data available makes it difficult to develop, apply, and validate theoretical models of the Port of Astoria. Consequently, the model results herein presented must be considered approximate. In spite of this, however, it should not be assumed that the models are of no value. The results of the

aerial photography, for example, do tend to confirm the flow patterns predicted by the physical model, at least over the incoming tide (see section VI B).

Field research efforts for this project were limited by the time, money, manpower, and equipment available. Considerable scope therefore remains for further on-site research efforts. In particular, further study of the following items would be highly desirable:

(a) Actual flushing rates experienced in both slips.

(b) Velocity distributions along both the length and depth of each slip.

(c) Suspended sediment concentrations as a function of time, river discharge and tidal cycle.

(d) Historical rates of sediment build-up based on soundings, dredging records, etc.

(e) The effect of commercial activities on the suspended and bottom sediments. It was observed that the movement of shipping and harbor tugs in slip number one caused considerable turbulence and, apparently, mobilized substantial quantities of bottom material into suspension. The effect of this "pulse" with very high concentrations of suspended sediments may warrant further investigation.

In conclusion, it is felt that the research detailed in this paper does serve to provide an understanding of the circulation and shoaling characteristics at the Port of Astoria. In order to further validate and refine these basic results, further reaearch efforts in the field are recommended.

References

1. Abraham, Gerritt, Hydraulic Far-Field Modeling, European Course on Heat Disposal from Power Generation in the Water Environment, Delft Hydraulics Laboratory, Delft, Netherlands, June 1975.

2. American Society of Civil Engineers, Manual of Engineering Practice No. 25, Hydraulic Models, ASCE, NY, NY, 1942.

3. Bennet & Myers, Momentum, Heat, and Mass Transfer, McGraw-Hill Incorporated, New York, 1962.

4. Bogardi, Janos, Sediment Transport in Alluvial Streams , Akademiai Kiado, Budapest, 1974.

5. Burgess, Fred J., and James, Wesley P., Airphoto Analysis of Ocean Outfall Dispersion, EPA Water Pollution Control Research News, No. 16070 ENS, June 1971.

6. Crickmore, M. J., Tracer Tests of Eddy Diffusion in Field & Model, J. Hydraul. Div, Proc. ASCE, Vol 98 (1972).

7. Dyer, K.R., Estuaries: A Physical Introduction, John Wiley & Sons, London, 1973.

8. Everts, C.H., A Method to Forecast Sedimentation Rates Resulting from the Settlement of Suspended Solids Within Semienclosed Harbors , Coastal Emergency Tech. Aid No. 81-6, U.S. Army Corps of Engineers Coastal Engineering Research Center, June 1981.

9. Fischer, Hugo B., Mixing in Inland and Coastal Waters, Academic Press, New York, 1979.

10. Fischer, Hugo B., & Holley, E. R., Analysis of the Use of Distorted Hydraulic Models for Dispersion Studies, Water Resources Research, American Geophysical Union, Vol. 7, No. 1, Feb. 1971.

11. Gelfenbaum, Guy, Suspended Sediment Response to Semi-Diurnal and Fortnightly Tidal Variations in a Mesotidal Estuary: Columbia River, U.S.A. University of Washington, Seattle, WA, 1982 (unpublished).

12. Hamilton, Stanley F., Oregon Estuaries, Oregon State Land Board, Salem, OR, 1973.

13. Ippen, A.T., Estuary &Coastline Hydrodynamics , McGraw-Hill, NY, 1966.

14. Krone, R. B., Investigation of the Causes of Shoaling in Slips One and Two, Port of Astoria, Unpublished report to the Port of Astoria, 1971.

15. Mc Dougal, W. G., 1-Dimensional Marina Flushing Model, Unpublished report, Oregon State University, Corvallis, OR, 1980.

16. Neal, Victor Thomas, A Calculation of Flushing Times and Pollution Distribution for the Columbia River Estuary, Ph.D. thesis in Oceanography, Oregon State University, 1965.

17. Slotta, L. S. & Tang, S. S., Chetco River Tidal Hydrodynamics and Associated Marina Flushing, Dept. of Ocean Engineering, Oregon State Univ., Sept. 1976.

18. Smart, P. L., & Laidlaw, I. M. S., An Evaluation of Some Fluorescent Dyes for Water Tracing, Water Resources Research, Vol. 73, No. 1, Feb. 1977.

19. Turner Designs Monograph, Flow Measurements, Turner Designs, Mountain View, CA, Nov. 1975.

20. U.S. Geological Survey, Water Data Report OR-80-2, Vol. 2, (Western Oregon), 1981.

21. Wright, F. F., Estuarine Oceanography, American Geological Institute, 1974.

22. Yotsukura, N. & Kilpatrick, F. A., Tracer Simulation of Soluble Waste Concentration, Journal of the Environmental Engineering Division, ASCE, Vol. 99, No. EE4, Aug. 1973.

Appendix A

FORTRAN Program for Numerical Circulation Model

```
      PROGRAM CONC(INPUT,TAPE5=INPUT,OUTPUT,TAPE6=OUTPUT,
     .CONOUT,TAPE7=CONOUT,DATA4,TAPE8=DATA4)
      DIMENSION U(10),L(10),H(10),Q(10),S(10)
      DIMENSION M(10),C(10,2),VR(10)
      REAL M,L
C*
C*
C*    INPUT DATA
C*
      AMPTID  = 6.9
      FREQ    = (2.0*3.14159)/(12.4*3600.0)
      DT      = 60.0
      RUNTME  = 1000.
      PRTTME  = 10.0
      SRCTME  = 1000.0
      NUMGRD  = 6
C*
C*    AMPTID  - TIDAL AMPLITUDE (FT)
C*    FREQ    - TIDAL FREQUENCY (1/SEC)
C*    DT      - TIME STEP (SEC)
C*    RUNTME  - RUN TIME (HR)
C*    PRTTME  - PRINT TIME INTERVAL (HR)
C*    SRCTME  - SOURCE TIME (HR)
C*                NO SOURCE          SRCTME=0.0
C*                FINITE SOURCE      SRCTME LESS THAN RUNTIME
C*                CONTINUOUS SOURCE  SRCTME=RUNTME
```

```
C*
C*    INITIAL AND BOUNDARY CONDITIONS
C*
      M(1)    = 0.0
      M(2)    = 0.0
      M(3)    = 0.0
      M(4)    = 0.0
      M(5)    = 0.0
      M(6)    = 0.0
      M(7)    = 0.0
      M(8)    = 0.0
      M(9)    = 0.0
      M(10)   = 0.0
      C(1,1)  = 0.0
      C(2,1)  = 0.0
      C(3,1)  = 0.0
      C(4,1)  = 0.0
      C(5,1)  = 0.0
      C(6,1)  = 0.0
      C(7,1)  = 0.0
      C(8,1)  = 0.0
      C(9,1)  = 0.0
      C(10,1) = 0.0
      S(1)    = 0.0
      S(2)    = 100.0
      S(3)    = 0.0
      S(4)    = 0.0
      S(5)    = 0.0
      S(6)    = 0.0
      S(7)    = 0.0
      S(8)    = 0.0
      S(9)    = 0.0
      S(10)   = 0.0
C*
C*    M       - QUANTITY OF TRACER (UNITS ARBRITARY)
C*    C       - TRACER CONCENTRATION (UNITS /FT**3)
C*    S        - SOURCE (UNITS/HR)
C*
C*    A NUMBER OF RUN OPTIONS ARE POSSIBLE.
C*      INPUT M             ZERO ENTERIES FOR C AND S
C*      INPUT C           ZERO ENTERIES FOR M AND S
C*      INPUT M AND S     ZERO ENTERIES FOR C
C*      INPUT C AND S     ZERO ENTERIES FOR M
C*      INPUT S           ZERO ENTERIES FOR M AND C
C*    THE PROGRAM WILL DETERMINE THE APPROPRIATE INITIAL CONDITIONS
C*    FROM THE RUN OPTION SELECTED.
```

```
C*
C*    GRID SPECIFICATIONS
C*
      W(1)=0.0
      W(2)=3440.0
      W(3)=3115.0
      W(4)=2620.0
      W(5)=1970.0
      W(6)=3440.0
      W(7)=0.0
      W(8)=0.0
      W(9)=0.0
      W(10)=0.0
      L(1)=0.0
      L(2)=4590.0
      L(3)=7870.0
      L(4)=8855.0
      L(5)=5740.0
      L(6)=9840.0
      L(7)=0.0
      L(8)=0.0
      L(9)=0.0
      L(10)=0.0
      H(1)=150.0
      H(2)=71.3
      H(3)=98.4
      H(4)=98.4
      H(5)=62.3
      H(6)=49.2
      H(7)=0.0
      H(8)=0.0
      H(9)=0.0
      H(10)=0.0
C*
C*    L       - LENGTH
C*    W       - WIDTH
C*    H       - DEPTH
C*
```

```
C*********************************************************************
C*
      DO 50I=1,10
   50 VR(I)=0.0
      DO 200I=1,9
      DO 100J=I,9
      K=J+1
      VR(I)=VR(I)+AMPTID*W(K)*L(K)
  100 CONTINUE
  200 CONTINUE
C*    VR       - VOLUME RATIO FOR FLOWS
      TEST1=0.0
      TEST2=0.0
      DO 300I=1,9
      TEST1=M(I)+TEST1
  300 TEST2=C(I,1)+TEST2
      IF(TEST2.EQ.0.0)GO TO 500
      DO 400I=2,9
  400 M(I)=C(I,1)*W(I)*L(I)*H(I)
      GO TO 760
  500 CONTINUE
      DO 600I=2,NUMGRD
  600 C(I,1)=(M(I))/(W(I)*L(I)*H(I))
  760 CONTINUE
      ETA1=0.0
      TIME=0.0
      DO 780I=1,10
  780 Q(I)=VR(I)*FREQ
      CALL OUT1(10,TIME,AMPTID,ETA1,M,C,S,Q)
```

```
C*
C*
      NTME=3600.0*RUNTME/DT+0.5
      NPRT=3600.0*PRTTME/DT+0.5
      SRC=1.0
      DO 1600J=1,NTME
      TIME=J*DT
      ETA2=AMPTID*SIN(FREQ*TIME)
      IF(SRCTME .GT. TIME)SRC=0.0
      DO 800I=1,9
  800 Q(I)=VR(I)*FREQ*COS(FREQ*TIME)
      S(I)=S(I)*SRC
      TEST=COS(FREQ*TIME)
      IF(TEST.LT.0.0)GO TO 1000
      DO 900I=2,NUMGRD
      A1=W(I)*L(I)*(H(I)+ETA1)
      A2=W(I)*L(I)*(H(I)+ETA2)
  900 C(I,2)=(1.0/A2)*((C(I-1,1)*Q(I-1)-C(I,1)*Q(I)+
     .S(I)/3600.)*DT+A1*C(I,1))
      GO TO 1200
 1000 CONTINUE
      DO 1100I=2,NUMGRD
      A1=W(I)*L(I)*(H(I)+ETA1)
      A2=W(I)*L(I)*(H(I)+ETA2)
      Q1=ABS(Q(I))
      Q2=ABS(Q(I-1))
 1100 C(I,2)=(1.0/A2)*((C(I+1,1)*Q1-C(I,1)*Q2+
     .S(I)/3600.)*DT+A1*C(I,1))
 1200 CONTINUE
      DO 1300I=2,NUMGRD
      H(I)=C(I,2)*(W(I)*L(I)*(H(I)+ETA2))
 1300 C(I,1)=C(I,2)
      ETA1=ETA2
      KK=AMOD(FLOAT(J),FLOAT(NPRT))
      IF(KK.EQ.0)CALL OUT1(NUMGRD,TIME,AMPTID,ETA1,H,C,S,Q)
 1600 CONTINUE
      END
C*
C*
```

```
C*
C*
      SUBROUTINE OUT1(NUMGRD,TIME,AMPTID,ETA,M,C,S,Q)
      DIMENSION M(10),C(10,2),S(9),Q(10)
      REAL M
      TH=TIME/3600.0
      WRITE(7,100)TH,AMPTID,ETA
  100 FORMAT(///2X,'TIME=',F6.3,4X,'TIDAL AMPLITUDE=',F6.3,4X,
     .'TIDAL HEIGHT',F7.3/)
      WRITE(7,200)
  200 FORMAT(1X,'GRID',7X,'MASS',9X,'CONC',9X,'SOURCE',8X,'FLOW')
      DO 300I=1,NUMGRD
  300 WRITE(7,400)I,M(I),C(I,1),S(I),Q(I)
  400  FORMAT(2X,I2,2X,E12.5,2X,E12.5,2X,E12.5,2X,E12.5)
      SUM=0.0
      DO 500I=1,NUMGRD
      SUM=M(I)+SUM
  500 CONTINUE
      WRITE(7,600)SUM
  600 FORMAT(2X,'TOTAL MASS',2X,E12.5)
      WRITE(8,800)TH,M(2),M(3),SUM
  800 FORMAT(F5.0,2X,E12.5,2X,E12.5,2X,E12.5)
      RETURN
      END
```

Appendix B

Calculating the Required Quantity of Dye for Field Exercises

Field tests using fluorescent dye tracers may be used to verify the results of the one-dimensional circulation model discussed in Section III. One decision which must be made prior to the field study is the quantity of tracer to be released. The required amounts can be estimated by assuming that the concentrations predicted by the model are approximately correct, then adding a safety factor to ensure that measurable readings can be obtained in the field.

The following example illustrates the method. The calculations were performed to determine the required quantities of tracer to be released in Slip #1 at the Port of Astoria.

A. "Slug Input": Assume that the fluorescent tracer is introduced as an instantaneous slug in the landward end of Slip #1. The low tide volume of the last cell in the model is:

$$V = WLH = (267.4 \text{ ft})(300 \text{ ft})(10 \text{ ft}) = 802{,}500 \text{ ft}^3 \quad (22800 \text{ m}^3)$$

Rounding the volume to 10^6 ft ^{3} ($28{,}300$ m^3), the initial concentration, Co, may be calculated as follows:

$$Co = V_{tracer}/(10^6 \text{ ft}^3)$$

The model predicts a residual concentration of 1% of Co in the seaward end of the slip after 100 hours. The following concentration may therefore be expected per gallon (3.8 l) of tracer released:

Initial Concentration (last cell)	Residual Concentration (first cell)
.1 ppm	.001 ppm

B. "Trickle Input": Assume that the dye is introduced continuously into the rear end of the slip. The predicted concentration at the mouth of the slip after 100 hours is on the order of 3×10^{-6} times the rate of input (units/hour). Consequently, the resulting concentration at the mouth of the slip would be about 0.5 ppm per gallon (3.8 liters) of tracer per hour.

Mc Dougal (1980) has noted that the model sometimes tends to underpredict flushing, particularly near the back end of the estuary. It therefore seems advisable to allow a one order of magnitude safety factor in determining the amount of dye to be released.

Finally, consider the sensitivity of the fluorometer. For the Turner Designs Model 10 Fluorometer used in the field exercise at the Port of Astoria, the preferred range of concentrations for measuring Rhodamine WT is from about .001 ppm to 1.0 ppm. (Turner Designs Monograph, 1975). Measurement may be accurate as low as 2 parts per trillion however, and concentrations higher than 1.0 ppm may be measured by diluting the sample prior to placing it in the fluorometer. To achieve residual concentrations within this range,

the tracer input should be as follows:

Method	Est. Resid. Conc./gal[1]	Required input
Slug	.0001 ppm	100 gal (380 l)
Trickle	.5 ppm	.1 gal/hr (.38 l/hr)

(1) incorporating a safety factor of 10.

Appendix C

FORTRAN Program for Numerical Sedimentation Model

```
      PROGRAM SHOAL (INPUT,OUTPUT,TAPE5=INPUT,TAPE6=OUTPUT)
      DIMENSION VS(10),CH(10),CR(10),M(10),D(10),MD(10),MOUT(10),MIN(10)
      REAL VS,MV,DT,AMPTID,FREQ,A,CH,CR,DEPTH,H,M,VOLDEP,DSHOAL,
     1TIME,VOL,ETA1,ETA2,DETA,Q,MDTOT,D,MD,VD,SHL,MOUT,MIN
      INTEGER NUMSIZ,NUMSTP,PRTTME
C
C *** INPUT DATA
C
C     NUMSIZ - NUMBER OF SIZE FRACTIONS FOR SEDIMENT
C     VS(N) - SETTLING VELOCITY FOR SIZE FRACTION N
C     MV - MASS OF SEDIMENT PER UNIT VOLUME OF DEPOSITION
C
C     DT - LENGTH OF TIME STEP, MINUTES
C     NUMSTP - NUMBER OF TIME STEPS IN RUN
C     PRTTME - NUMBER OF TIME STEPS BETWEEN PRINTOUTS
C
C     AMPTID - TIDAL AMPLITUDE
C     FREQ - TIDAL FREQUENCY,RADIANS/MINUTE
C
C     A - HARBOR SURFACE AREA
C
      NUMSIZ = 1
      VS(1) = 0.12
      VS(2) = 0.0
      VS(3) = 0.0
      VS(4) = 0.0
      VS(5) = 0.0
      VS(6) = 0.0
      VS(7) = 0.0
      VS(8) = 0.0
      VS(9) = 0.0
      VS(10)= 0.0
      MV = 44.9
      DT =31.0
      NUMSTP = 1392
      PRTTME = 12
      AMPTID = 5.0
      FREQ = (2.0*3.14159)/(12.4*60.0)
      A = 363000.0
```

```
C
C *** INITIAL AND BOUNDARY CONDITIONS
C
C     CH(N) = AVERAGE CONC IN HARBOR OF SIZE FRACTION N
C     CR(N) = AVERAGE CONC IN RIVER OF SIZE FRACTION N
C     DEPTH = AVERAGE HARBOR DEPTH RELATIVE TO MLLW
C     H = DEPTH OF WATER IN HARBOR
C     M(N) = MASS OF SIZE FRACTION N IN HARBOR
C     VOLDEP = CUMULATIVE VOLUME OF SEDIMENT DEPOSITED
C     DSHOAL = CUMULATIVE DEPTH OF SHOALING
      CH(1) = 1.3E-3
      CH(2) = 0.0
      CH(3) = 0.0
      CH(4) = 0.0
      CH(5) = 0.0
      CH(6) = 0.0
      CH(7) = 0.0
      CH(8) = 0.0
      CH(9) = 0.0
      CH(10)= 0.0
      CR(1) = 4.5E-2
      CR(2) = 0.0
      CR(3) = 0.0
      CR(4) = 0.0
      CR(5) = 0.0
      CR(6) = 0.0
      CR(7) = 0.0
      CR(8) = 0.0
      CR(9) = 0.0
      CR(10)= 0.0
      DEPTH = 20.0
      H = DEPTH+AMPTID
      TIME = 0.0
      VOL = H*A
      DO 10 N=1,NUMSIZ
   10 M(N) = CH(N)*VOL
      VOLDEP = 0.0
      DSHOAL = 0.0
```

```
   20 DO 100 I = 1,NUMSTP
C
C *** CALCULATE INFLOW/OUTFLOW
C
      ETA1 = AMPTID*SIN(FREQ*TIME)
      ETA2 = AMPTID*SIN(FREQ*(TIME+DT))
      DETA = ETA2-ETA1
      Q = DETA*A
C
C *** CALCULATE MASS OF SEDIMENT DEPOSITED
C
      MDTOT = 0.0
      DO 30, N = 1,NUMSIZ
      D(N) = (VS(N)*DT)
      IF (D(N).LE.H) GO TO 25
      URITE (6,21)
   21 FORMAT ("TIME INCREMENT EXCESSIVE FOR VS AND H")
      GO TO 110
   25 MD(N) = CH(N)*D(N)*A
      MDTOT = MDTOT+MD(N)
   30 CONTINUE
      VD = MDTOT/MV
      SHL = VD/A
C
C *** MASS OF SEDIMENT FLOWING IN/OUT OF HARBOR
C
      IF (Q.GT.0.0) GO TO 50
C
C *** OUTGOING TIDE
C
      DO 40 N = 1,NUMSIZ
      MOUT(N) = ((M(N)-MD(N))/VOL)*Q
      MIN(N) = 0.0
   40 CONTINUE
      GO TO 70
C
C *** INCOMING TIDE
C
   50 DO 60 N = 1,NUMSIZ
      MIN(N) = CR(N)*Q
      MOUT(N) =0.0
   60 CONTINUE
C
C *** MASS IN HARBOR AT END OF TIME SEGMENT
C
   70 DO 80 N = 1,NUMSIZ
      M(N) = M(N) + MIN(N) + MOUT(N) - MD(N)
   80 CONTINUE
```

```
C
C *** ADJUST DEPTH AND VOLUME IN HARBOR
C
      DEPTH = DEPTH-SHL
      H = H-SHL+DETA
      VOL = A*H
C
C *** CONCS IN HARBOR AT END OF TIME SEGMENT
C
      DO 90 N = 1,NUMSIZ
      CH(N) = M(N)/VOL
   90 CONTINUE
C
C *** UPDATE TIME
C
      TIME = TIME+DT
C
C *** CUMULATIVE VOLUME DEPOSITED AND DEPTH OF SHOALING
C
      VOLDEP = VOLDEP+VD
      DSHOAL = DSHOAL+SHL
C
C *** IF PRTTME GO TO SUBROUTINE OUT
C
      KK = MOD(I,PRTTME)
      IF (KK.EQ.0) CALL OUT (TIME,VOLDEP,DSHOAL)
  100 CONTINUE
  110 STOP
      END
C
C
C ***************************************************************
C
C
      SUBROUTINE OUT (TIME,VOLDEP,DSHOAL)
      REAL TIME,VOLDEP,DSHOAL,TH
      TH = TIME/60.0
      WRITE (6,200) TH,VOLDEP,DSHOAL
  200 FORMAT (F10.3,E12.5,E12.5)
      RETURN
      END
```

Appendix C (continued)

Input parameters for numerical sedimentation model runs:

Run 1

NUMSIZE = 1

VS(1) = .06 ft/min

VS(2) - VS(10) = 0.0

MV = 44.9 lbs/ft^3

AMPTID = 5.0 ft

CH(1) = 1.3×10^{-3} lbs/ft^3

CH(2) - CH(10) = 0.0

CR(1) = 4.5×10^{-3} lbs/ft^3

CR(2) - CR(10) = 0.0

Run 2

All parameters equal to those in Run 1 except

VS(1) = .12 ft/min

Run 3

All parameters equal to those in Run 2 except

CR(1) = 4.5×10^{-2} lbs/ft^3

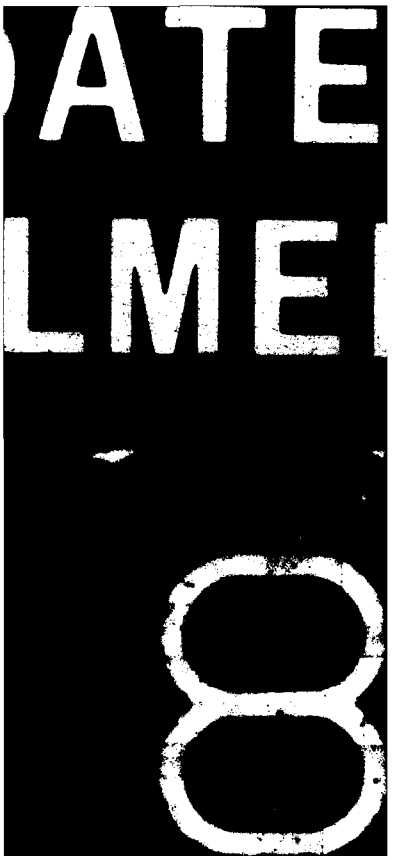
ATE
LME
8